A new average wave overtopping prediction formula with improved accuracy for smooth steep low-crested structures

David Gallach-Sánchez [a,b,*], Peter Troch [b], Andreas Kortenhaus [b]

[a] DEME Group, Haven 1025 - Scheldedijk 30, 2070, Zwijndrecht, Belgium
[b] Dept. of Civil Engineering, Ghent University, Technologiepark 60, 9052, Zwijnaarde, Belgium

ABSTRACT

Wave overtopping is a key process in coastal protection and its assessment defines the design of the sea defence structures. An existing knowledge gap in wave overtopping prediction is identified for steep low-crested structures, i.e., structures with steep slopes up to the limit case of vertical structures, with small relative freeboards down to the limit case of zero freeboards. This type of structure is increasingly relevant in a sea level rise context due to climate change. Additionally, steep low-crested structures are also of interest when used as overtopping wave energy converters. To cover the identified knowledge gap, more than 900 2D hydraulic model tests have been performed in the wave flume of the Department of Civil Engineering at Ghent University. Wave conditions and the overtopping performance have been measured. After analysing the average overtopping rates of the new tests, we found that there is a lack of accuracy of the recommended EurOtop 2018 manual overtopping prediction formulae for steep low-crested structures. Based on the new tests, a new average overtopping prediction formula for steep low-crested structures is obtained. This formula improves the prediction accuracy of the average overtopping rates for steep low-crested structures with respect to the recommended predictions in the EurOtop 2018 manual by reducing the RMSE by 35% for zero freeboards, by 16% for very small relative freeboards, by 31% for very steep slopes and by 24% for vertical structures. The accuracy of the EurOtop 2018 manual predictions for other structural types is maintained.

1. Introduction

Wave overtopping is a key process in the design of sea defence structures. The overtopping events occurring during wave attack pose a threat to human lives, damage of property and infrastructure, and economic losses. A good knowledge of the wave overtopping process is necessary to improve the safety of sea defence structures. A type of sea defence structures which only recently became subject of investigation is the steep low-crested structures. This type refers to structures with slope angles from mild to vertical ($2 > \cot \alpha \geq 0$) and relative crest freeboards from small to zero ($0.8 > R_c/H_{m0} \geq 0$).

In a climate change context with sea levels rising globally and an increased storminess (i.e., more frequent and severe storms), the existing sea defence structures are becoming low-crested structures. Therefore, improved knowledge regarding the overtopping process is important to assess the safety of the existing coastal structures and to update the existing design guidelines. The steep and very steep structures are interesting to study as a limit case with vertical structures, which have been used widely as defence structures.

The steep low-crested structures are not only of importance as sea defence structures. The overtopping wave energy converter (OWEC) is a type of wave energy device that captures the overtopped water over a structure in a reservoir. The reservoir is emptied by a set of low-head turbines, generating electricity. Higher overtopping rates result in greater energy generation potential. The steep low-crested structures maximize the overtopping rates and therefore are of interest for OWECS applications (Gallach-Sánchez et al., 2018).

A knowledge gap of wave overtopping for steep low-crested structures was identified by Victor and Troch (2012a), which they partially filled by performing 2D physical model tests at Ghent University (Belgium), obtaining the so-called UG10 dataset (Victor and Troch, 2012b). The UG10 dataset includes overtopping data for slope angles $2.75 \geq \cot \alpha \geq 0.36$, and relative crest freeboards $1.69 \geq R_c/H_{m0} \geq 0.11$. However, this dataset did not include tests for very steep slopes ($0.36 > \cot \alpha > 0$) and vertical structures ($\cot \alpha = 0$), combined with very small relative crest freeboards ($0.11 \geq R_c/H_{m0} > 0$)

* Corresponding author. DEME Group, Haven 1025 - Scheldedijk 30, 2070, Zwijndrecht, Belgium.
  E-mail address: Gallach.Sanchez.David@deme-group.com (D. Gallach-Sánchez).

Table 1
Range definition of slope angle α.

	cot α [−]
Mild slopes	cot α > 1.5
Steep slopes	1.5 ≥ cot α > 0.27
Very steep slopes	0.27 ≥ cot α > 0
Vertical structures	cot α = 0

Table 2
Range definition of relative crest freeboard R_c/H_{m0}.

	Relative crest freeboard R_c/H_{m0} [−]
Large relative crest freeboard	$R_c/H_{m0} \geq 0.8$
Small relative crest freeboard	$0.8 > R_c/H_{m0} \geq 0.11$
Very small relative crest freeboard	$0.11 > R_c/H_{m0} > 0$
Zero crest freeboard	$R_c/H_{m0} = 0$

and zero freeboards ($R_c = 0$). Based on the UG10 dataset and data available in the CLASH database (De Rouck et al., 2009), two average overtopping prediction formulae were obtained by Victor and Troch (2012a) and Van der Meer and Bruce (2014), the latter being included in the latest update of the EurOtop (2018) manual. The accuracy of these prediction formulae is good for the range of the UG10 dataset. However, an improvement of the prediction accuracy is still possible (Gallach-Sánchez et al., 2018) for very steep slopes to vertical structures with very small to zero relative crest freeboards, which is further proved in the present paper.

The aim of this research is to obtain a new average overtopping prediction formula that improves the accuracy of existing prediction formulae for the range of steep low-crested structures, especially the Van der Meer and Bruce (2014) prediction as it is the reference prediction in the EurOtop (2018) manual. To achieve this aim, 2D physical model tests were performed at Ghent University (Belgium), obtaining 939 overtopping tests resulting in the so-called UG13, UG14 and UG15 datasets. These tests were analysed and a new average overtopping prediction formula is obtained and presented in this paper. This new

prediction formula is fitted through the new datasets and through relevant parts of the CLASH database (De Rouck et al., 2009). This paper is based on the outcomes of the doctoral research by Gallach-Sánchez (2018).

The definition ranges of slope angle *α* and relative crest freeboard R_c/H_{m0} that are used in this paper are shown in Table 1 and Table 2, respectively.

Section 2 presents a literature review of the overtopping for steep low-crested structures including the existing prediction formulae valid for this type of structures. Section 3 explains the experimental setup and the test programme of the 2D physical model tests performed at Ghent University. Section 4 compares the new Ghent University overtopping data with the existing overtopping prediction formula for steep low-crested structures. Section 5 proposes a new average overtopping prediction formula for steep low-crested structures based on new and existing overtopping data. Finally, Section 6 presents the conclusions of this research.

2. Overview of average overtopping prediction formulae

While the study of the wave overtopping process for common types of coastal structures (i.e., mild slopes with large relative freeboards) is widely covered in the scientific literature, for some structural types like steep low-crested structures there are knowledge gaps to be addressed. A selection of the most relevant average wave overtopping prediction formulae are reviewed in this section.

2.1. Mild sloping structures

The EurOtop (2007) manual includes Eq. (1) by Van der Meer and Janssen (1994) as the recommended average overtopping prediction the formula for mild sloping structures under non-breaking conditions (maximum average overtopping rate):

$$\frac{q}{\sqrt{gH_{m0}^3}} = 0.2 \exp\left[-2.6\frac{R_c}{H_{m0} \cdot \gamma_f \cdot \gamma_\beta}\right] \tag{1}$$

where q [m³/s/m] is the average overtopping rate, H_{m0} [m] is the incident spectral wave height at the toe of the structure, R_c [m] is the
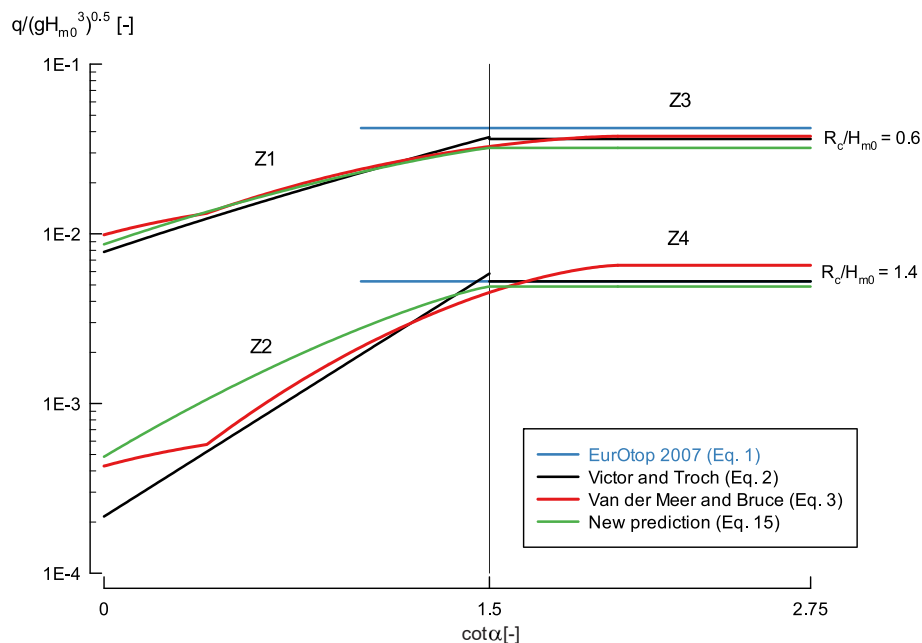

Fig. 1. Average overtopping prediction formulae by EurOtop (2007) (Eq. (1)), Victor and Troch (2012a) (Eq. (2)), Van der Meer and Bruce (2014) (Eq. (3)) and the new prediction (Eq. (15)) as a function of the slope *cot α* for two selected values of the relative crest freeboard $R_c/H_{m0} = 0.6$ and $R_c/H_{m0} = 1.4$.
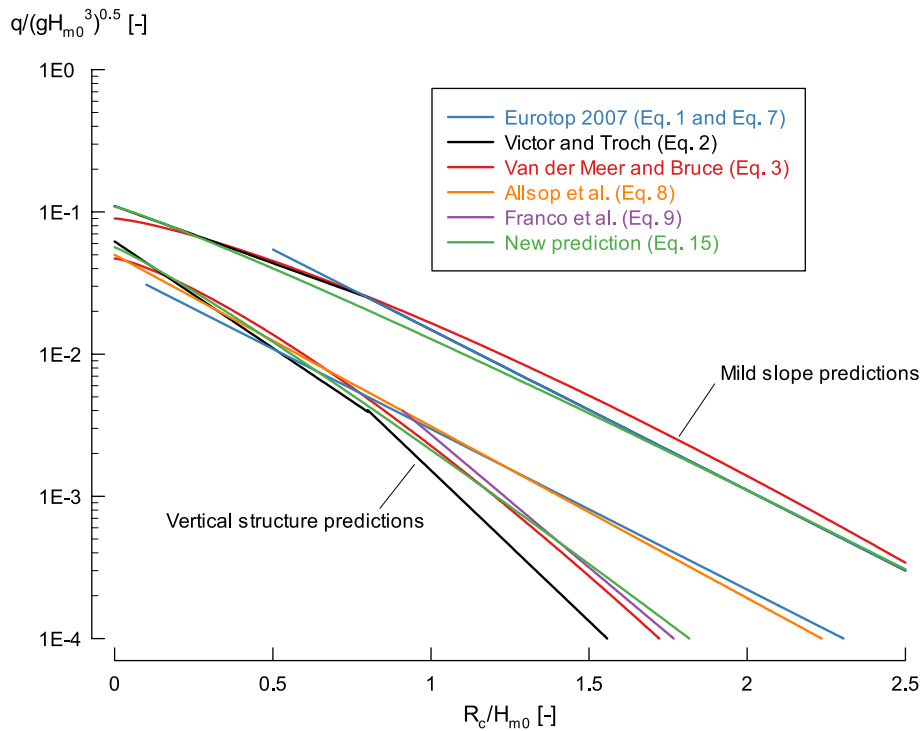
Fig. 2. Average overtopping prediction formulae by EurOtop (2007) (Eq. (1) for mild sloping structures and Eq. (7) for vertical structures), Victor and Troch (2012a) (Eq. (2)), Van der Meer and Bruce (2014) (Eq. (3)), Allsop et al. (1995) (Eq. (8)), Franco et al. (1994) (Eq. (9)) and the new prediction (Eq. (15)) as a function of the relative crest freeboard R_c/H_{m0} for mild slopes ($cot\ \alpha > 2$) and vertical structures ($cot\ \alpha = 0$).

crest freeboard and $\gamma_f, \gamma_\beta\ [-]$ are the influence factors for the roughness of the slope and oblique wave attack, respectively. The formula was fitted through a set of overtopping data including subsets of the CLASH database (De Rouck et al., 2009) and various datasets published in the TAW (2002) report. The exponent 2.6 of Eq. (1) is a normally distributed stochastic parameter with an associated standard deviation of $\sigma = 0.35$.

While this prediction is valid for the most common types of sea defence structures under non-breaking conditions, it leaves out of its application range the steep low-crested structures that are of interest for certain applications as explained in Section 1. Eq. (1) is only valid for mild sloping structures ($1 \leq cot\ \alpha \leq 4$) with large to small relative crest freeboards ($0.5 \leq R_c/H_{m0} < 3.5$) under non-breaking conditions. Even though this prediction formula is not valid for the range of steep low-crested structures, its analysis is valuable as limit case for steep low-crested structures.

Eq. (1) is not dependent on the slope angle α (see Fig. 1). The shape of Eq. (1) is linear in a semilogarithmic plot of the dimensionless average overtopping rate $q/\sqrt{gH_{m0}^3}\ [-]$ against the relative crest freeboard $R_c/H_{m0}\ [-]$ (see Fig. 2).

2.2. Steep low-crested structures

2.2.1. Victor and Troch (2012a)

Victor and Troch (2012a) developed a new formula within the PhD research of Victor (2012) about the operational conditions of OWECs, which feature steep low-crested structures (see Section 1):

$$\frac{q}{\sqrt{gH_{m0}^3}} = a_{Victor} \cdot exp\left[- b_{Victor} \cdot \frac{R_c}{H_{m0}} \right] \qquad (2)$$

This formula was fitted through the UG10 dataset (Victor and Troch, 2012b) and the subsets 106, 107 and 402 of the CLASH database (all of them for plain vertical structures under non-impulsive conditions with a relative crest freeboards $R_c/H_{m0} < 0.8$). Depending of the values of slope

Table 3

Coefficients of Victor and Troch (2012a) prediction formulae (Eq. (2)) as a function of the slope angle α and relative crest freeboard R_c/H_{m0}.

		Relative crest freeboard R_c/H_{m0}			
		$0 \leq R_c/H_{m0} \leq 0.8$		$0.8 \leq R_c/H_{m0} \leq 2$	
Slope $cot\ \alpha$	$0 \leq cot\ \alpha \leq 1.5$	Z1	$a_{Victor} = 0.033$ $\cdot cot\ \alpha + 0.062$ $b_{Victor} = 3.45 -$ $1.08 \cdot cot\ \alpha$	Z2	$a_{Victor} = 0.2$ $b_{Victor} = 4.88 -$ $1.57 \cdot cot\ \alpha$
	$1.5 \leq cot\ \alpha \leq 2.75$	Z3	$a_{Victor} = 0.11$ $b_{Victor} = 1.85$	Z4	$a_{Victor} = 0.2$ $b_{Victor} = 2.6$

angle α and relative crest freeboard R_c/H_{m0}, the formula is divided into four different zones, providing a high physical insight of the influence of these parameters on the overtopping prediction. Eq. (2) shows the formula (mean value approach) to predict the dimensionless average overtopping rate $q/\sqrt{gH_{m0}^3}$ and Table 3 shows the expressions for the a_{Victor} and b_{Victor} coefficients as a function of the slope angle α and relative crest freeboard R_c/H_{m0}. The range of application of the prediction formula is defined for slope angles $2.75 \geq cot\ \alpha \geq 0$ with relative crest freeboards $2 \geq R_c/H_{m0} \geq 0$.

For (very) steep slopes, the effect of the slope angle α on wave overtopping is significant, being stronger for larger freeboards (zone Z2) than for smaller freeboards (zone Z1). For milder slopes (zones Z3 and Z4), the effect of the slope angle α on wave overtopping is negligible and therefore not considered in the coefficients, which is in agreement with the EurOtop (2007) manual prediction. Moreover, the coefficients in the zone Z4 are equal to those in Eq. (1). Fig. 1 shows graphically the influence of $cot\ \alpha$ on the overtopping prediction. The consequence of the division of the prediction into four different zones is the bilinear shape of the prediction in a semilogarithmic plot (Fig. 2).

The uncertainty of the Victor and Troch (2012a) prediction is estimated by using a so-called Overtopping Discharge Factor (ODF), based

on the root mean square error (RMSE) of the logarithms of the measured and predicted dimensionless average overtopping rates of the fitting dataset. The resulting expression of the ODF for the 90% confidence band is ODF = $10^{1.645 \cdot RMSE}$, which is applied to three of the four defined zones of overtopping (Z1 to Z3). The ODF for the zone Z1 is ODF = 1.25; for the zone Z2 is ODF = 1.47; and for the zone Z3 is ODF = 1.18. To obtain the upper limit of 90% confidence band, the predicted dimensionless overtopping rate should be multiplied by the ODF; while to obtain the lower limit 90% confidence band, it should be divided by the ODF. In the zone Z4 the Victor and Troch (2012a) prediction is equal to Eq. (1) and therefore the 90% confidence band is the same as Eq. (1) (standard deviation $\sigma = 0.35$ of the coefficient 2.6).

2.2.2. *Van der Meer and Bruce (2014)*

Van der Meer and Bruce (2014) also developed an average overtopping prediction formula valid for steep low-crested structures:

$$\frac{q}{\sqrt{gH_{m0}^3}} = a_{V\&B} \cdot exp\left(-\left(b_{V\&B}\frac{R_c}{H_{m0} \cdot \gamma_f \cdot \gamma_\beta}\right)^{c_{V\&B}}\right) \tag{3}$$

with the following expressions for the coefficients $a_{V\&B}$, $b_{V\&B}$ and $c_{V\&B}$:

$$a_{V\&B} = 0.09 - 0.01(2 - \cot\alpha)^{2.1} \text{ for } \cot\alpha \leq 2$$
$$\text{and } a_{V\&B} = 0.09 \text{ for } \cot\alpha > 2 \tag{4}$$

$$b_{V\&B} = 1.5 + 0.42(2 - \cot\alpha)^{1.5} \quad \text{for } \cot\alpha \leq 2,$$
$$\text{with a maximum of } b_{V\&B} = 2.35;$$
$$\text{and } b_{V\&B} = 1.5 \text{ for } \cot\alpha > 2 \tag{5}$$

$$c_{V\&B} = 1.3 \tag{6}$$

Gallach-Sánchez et al. (2018) did an analysis and validation of the prediction formula, determining that it was fitted through the UG10 dataset (as the Victor and Troch (2012a) prediction), the subsets 106, 107, 113, 228, 229, 315, 351, 380 and 914 of the CLASH database (De Rouck et al., 2009) and the EurOtop (2007) dataset.

The mean value approach of the Van der Meer and Bruce (2014) formula is presented in Eq. (3), and it depends on the slope angle α (see Fig. 1) and the relative crest freeboard R_c/H_{m0}. The range of application of the prediction formula is for slope angles $\cot\alpha \geq 0$ with relative crest freeboards $R_c/H_{m0} \geq 0$. The reliability of Eq. (3) is described by a coefficient of variation $\sigma' = \sigma/\mu$ (where σ is the standard deviation and μ the average value of the coefficient for a specific slope angle) for the coefficients $a_{V\&B}$ and $b_{V\&B}$ with the values $\sigma'(a_{V\&B}) = 0.15$ and $\sigma'(b_{V\&B}) = 0.1$. This prediction is included in the EurOtop (2018) manual as the reference overtopping prediction for structures with steep slopes up to vertical structures. For design purposes and safety assessment, the average overtopping prediction should be increased by one standard deviation (EurOtop, 2018).

In Eq. (3), the coefficient $a_{V\&B}$ determines the value of the dimensionless average overtopping rate $q/\sqrt{gH_{m0}^3}$ for the zero freeboard case ($R_c = 0$), while the coefficient $b_{V\&B}$ determines the shape of the prediction for the entire range of relative crest freeboards R_c/H_{m0}. Compared to Eq. (1) and Eq. (2), Eq. (3) adds a constant power coefficient $c_{V\&B}$ inside the exponential function, indicating that the prediction follows a Weibull distribution. This power value $c_{V\&B}$ results in a curved shape of the prediction in a semilogarithmic plot, compared to the straight line of Eq. (1) and the bilinear shape of Eq. (2) (see Fig. 2).

In the past, Battjes (1974) presented an analytical overtopping prediction formula for mild slopes with breaking wave conditions. While most of the existing predictions feature an exponential formula that on a semilogarithmic plot is a straight line, this prediction features a bivariate Rayleigh distribution which is a curve on a semilogarithmic plot. Two reformulations of the Battjes (1974) prediction were made: a first one in the TAW (1989), and a second one made by Van der Meer et al. (2013) to match the EurOtop (2007) overtopping prediction for

breaking waves. Combining both reformulations, Van der Meer et al. (2013) found that Battjes (1974) was adapting well to the CLASH data for large freeboards and, surprisingly, also to zero freeboard data (CLASH subset 102 by Smid (2001)).

Indeed, the curved shape of the prediction in a semilogarithmic plot fits the data for zero freeboard of the CLASH subset 102, which a straight line prediction would greatly overpredict. The same principle is followed by Van der Meer and Bruce (2014) in the fitting of their prediction: a curved line on a semilogarithmic plot would accurately predict the overtopping for large relative crest freeboard and the very small and zero freeboards. The three-parameter Weibull distribution is chosen by Van der Meer and Bruce (2014) with a $c = 1.3$.

The roughness influence factor γ_f and the oblique wave attack influence factor γ_β to be used in Eq. (3) are shown in the EurOtop (2018) manual. However, these factors were obtained for Eq. (1) (EurOtop, 2007), meaning that they were fitted with an exponent $c = 1.0$ and are not within the part of the $c = 1.3$ in the formula. Therefore, its use with an exponent $c = 1.3$ (such as Eq. (3)) is mathematically incorrect (Van der Werf and Van Gent, 2018; Van Gent and Van der Werf, 2019). The differences between Eq. (1) and Eq. (3) are estimated in the EurOtop (2018) manual for any value of γ_f from +27% to −30%. These differences are within the 90% prediction band and, according to the EurOtop (2018) manual, are insignificant. However, the use of the published γ_f and γ_β factors can produce large differences in average overtopping absolute values, especially when increasing the average overtopping prediction by one standard deviation for design purposes.

2.3. *Limit cases for vertical structures and zero freeboard*

Vertical structures ($\cot\alpha = 0$) and zero freeboard structures ($R_c/H_{m0} = 0$) are the limit cases of steep low-crested structures. The Victor and Troch (2012a) (Eq. (2)) and Van der Meer and Bruce (2014) (Eq. (3)) prediction formulae are valid for vertical structures and zero freeboard structures, including these limit cases on the prediction of the overtopping for steep low-crested structures. However, both predictions were fitted through a limited number of tests with zero freeboard from Smid (2001). Hence, concerns about the accuracy of these overtopping predictions in this range arise (Gallach-Sánchez et al., 2018). Besides these predictions, various authors developed prediction formulae only valid for vertical structures or zero freeboards.

2.3.1. *Vertical structures*

Various average overtopping prediction formulae for the case of vertical structures ($\cot\alpha = 0$) are available in the scientific literature. The EurOtop (2007) manual presented Eq. (7) (with a standard deviation $\sigma(2.6) = 0.8$) as the average overtopping prediction for vertical structures under non-impulsive conditions, for a range of relative crest freeboards $0.1 \leq R_c/H_{m0} \leq 3.5$:

$$\frac{q}{\sqrt{gH_{m0}^3}} = 0.04 \exp\left[-2.6\frac{R_c}{H_{m0}}\right] \tag{7}$$

Allsop et al. (1995) presented Eq. (8) (with a standard deviation $\sigma(2.78) = 0.17$) for vertical structures under non-impulsive conditions valid for $R_c/H_{m0} \geq 0$, although with a best prediction range for relative crest freeboards $R_c/H_{m0} < 0.91$ according to Van der Meer and Bruce (2014):

$$\frac{q}{\sqrt{gH_{m0}^3}} = 0.05 \exp\left[-2.78\frac{R_c}{H_{m0}}\right] \tag{8}$$

In the EurOtop (2018) manual, the Allsop et al. (1995) formula (Eq. (8)) is the suggested prediction for vertical and composite vertical structures with influencing foreshores and non-impulsive (non-breaking) conditions, however, for the full range of R_c/H_{m0}. This prediction was fitted through data in relatively shallow water conditions.

Table 4
Summary of the overtopping prediction formulae.

Equation	Reference	Fitting datasets	cot α [−]	R_c/H_{m0} [−]
Eq. 1	EurOtop (2007) sloping structures non-breaking	CLASH	$1 \leq \cot \alpha \leq 4$	$0.5 \leq R_c/H_{m0} \leq 3.5$
Eq. 2	Victor and Troch (2012a)	CLASH and UG10	$0 \leq \cot \alpha \leq 2.75$	$0 \leq R_c/H_{m0} \leq 2$
Eq. 3	Van der Meer and Bruce (2014)	CLASH, UG10 and EurOtop (2007)	$\cot \alpha \leq 2.75$	$R_c/H_{m0} \geq 0$
Eq. 7	EurOtop (2007) vertical structures non-impulsive conditions	CLASH	$\cot \alpha = 0$	$0.1 \leq R_c/H_{m0} \leq 3.5$
Eq. 8	Allsop et al. (1995)	CLASH	$\cot \alpha = 0$	$R_c/H_{m0} \geq 0$
Eq. 9	Franco et al. (1994)	CLASH	$\cot \alpha = 0$	$R_c/H_{m0} \geq 0.91$
Eqs. (10) and (11)	Schüttrumpf (2001)	CLASH subsets 102 and 103	$\cot \alpha \geq 3$	$R_c/H_{m0} = 0$
Eq. 12	Smid (2001)	CLASH subset 107	$\cot \alpha = 0$	$R_c/H_{m0} = 0$

Franco et al. (1994) presented Eq. (9) (with a standard deviation $\sigma(4.3) = 0.6$) also for vertical structures under non-impulsive conditions:

$$\frac{q}{\sqrt{gH_{m0}^3}} = 0.2 \exp\left[-4.3\frac{R_c}{H_{m0}}\right] \tag{9}$$

The formula was fitted through tests with relatively deep water conditions and relative crest freeboards $R_c/H_{m0} > 0.91$, which matches the best prediction range of the formula according to Van der Meer and Bruce (2014). This prediction is not featured in the EurOtop (2018) manual.

In the EurOtop (2018) manual, the recommended overtopping prediction for vertical structures without an influencing foreshore is the Van der Meer and Bruce (2014) formula (Eq. (3)) particularized for vertical structures.

The comparison of all the prediction formulae valid for vertical structures ($\cot \alpha = 0$) is shown in Fig. 2. For small relative crest freeboards, all the formulae feature predictions within the same range. For large relative crest freeboards, the EurOtop (2007) prediction (Eq. (7)) and the Allsop et al. (1995) prediction (Eq. (8)) feature larger overtopping rates for the same values of relative crest freeboard.

2.3.2. Zero freeboard

For the zero freeboard case ($R_c/H_{m0} = 0$), Schüttrumpf (2001) developed two prediction formulae depending on the surf similarity parameter $\xi_{m-1,0}$ for breaking (Eq. (10)) and non-breaking (Eq. (11)) wave conditions:

$$\frac{q}{\sqrt{gH_{m0}^3}} = 0.0537 \cdot \xi_{m-1,0} \ for \ \xi_{m-1,0} < 2 \tag{10}$$

$$\frac{q}{\sqrt{gH_{m0}^3}} = 0.136 - \frac{0.226}{\xi_{m-1,0}^3} \ for \ \xi_{m-1,0} \geq 2 \tag{11}$$

These formulae were fitted through part of the CLASH subsets 102 and 103 for mild sloping structures ($\cot \alpha \geq 3$). Although for steep and very steep slopes these formulae are out of the application range, it is worth to calculate the prediction for these slopes for comparison purposes. The surf similarity parameter is $\xi_{m-1,0} > 10$ for steep and very steep slopes (due to the large values of $\tan \alpha$ of the slopes), which results in the Schüttrumpf (2001) being asymptotic to a constant value of $q/\sqrt{gH_{m0}^3} = 0.136$.

Smid (2001) developed a prediction (Eq. (12)) for vertical structures ($\cot \alpha = 0$) with zero freeboards ($R_c = 0$) based on part of the CLASH subset 107:

$$\frac{q}{\sqrt{gH_{m0}^3}} = 0.062 \pm 0.0062 \tag{12}$$

Table 4 presents a summary of the overtopping prediction formulae reviewed in this section with their range of application and the fitting datasets.

3. Experimental setup and test programme

Three new wave overtopping datasets—UG13, UG14 and UG15—-with a total of 939 tests were obtained to improve the knowledge of wave overtopping for steep low-crested structures. In this section, an overview of the experimental setup used in the model tests and a description of the test programme are presented.

3.1. Experimental setup

The 2D experiments were performed in the wave flume of the Department of Civil Engineering at Ghent University (Belgium). The wave flume has a length of 30 m, a width of 1 m and a height of 1.2 m (Fig. 3). The wave generation system consists of a piston type wave paddle with a maximum stroke length of 1.5 m, which can generate individual wave heights up to 0.35 m. It is equipped with an active wave absorption system that absorbs the reflected waves and simultaneously generates the desired wave time series.

The model structure tested in the wave flume consisted of a smooth impermeable plywood panel forming a slope angle α with the foreshore (Fig. 4). Behind the model structure an overtopping box was placed, containing the necessary equipment to measure wave overtopping. The overtopping box was developed by Victor and Troch (2010) to measure the average and individual wave overtopping. The method used is the load cell technique, consisting on measuring the weight of the overtopped water in a reservoir. If the total overtopping volume was exceeding the capacity of the reservoir, a pump was automatically activated, returning the overtopped water to the wave flume. The signal of the load cell was then postprocessed with a MATLAB™ script, obtaining the average wave overtopping rate of each test. To ensure that this method was measuring large overtopping rates with accuracy, the width of the overtopping chute that collects the water was reduced for
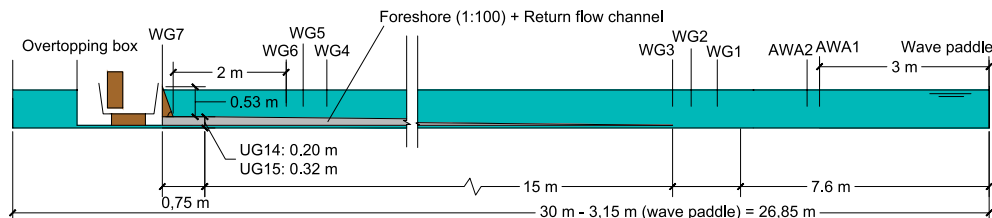

Fig. 3. Test setup of the UG14 and UG15 experiments (drawing not to scale).
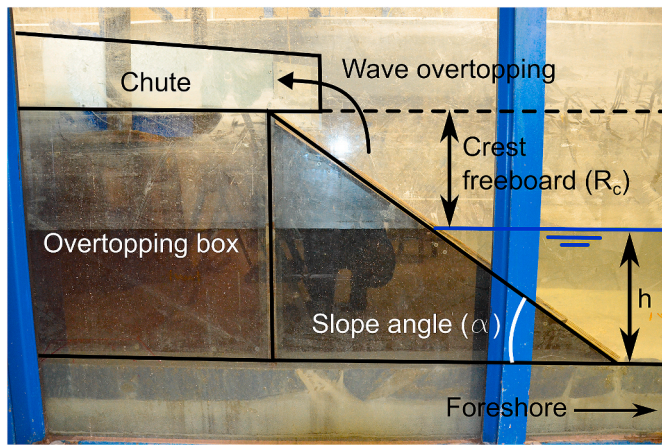
Fig. 4. Cross section of the model structure.

the tests were large overtopping rates were expected. No influence of the chute width on the average overtopping was observed. Moreover, the wave flume operator checked for every test that all the overtopped water was being collected in the overtopping reservoir. Repeatable overtopping results were found for small relative freeboards, with a coefficient of variation between $\sigma' = 2\%-5\%$ for different seeding numbers of the wave series (Gallach-Sánchez, 2018). This value of the coefficient of variation is lower than values reported in literature (Kortenhaus et al., 2004; Romano et al., 2015).

The foreshore of the wave flume was adapted for each dataset to minimize the construction costs. The UG13 dataset had a horizontal foreshore near the toe of the structure (Gallach-Sánchez et al., 2018), while the UG14 and UG15 datasets (Fig. 3) had a mild 1:100 foreshore slope over 15 m (Gallach-Sánchez et al., 2014, 2016). For all three datasets, the influence of the foreshore was negligible, as it did not modify the wave propagation processes. A return flow channel is constructed beneath the foreshore. The channel allowed the return of the overtopped water behind the model to the central part of the flume in order to have a constant water level, also for tests with the largest overtopping rates.

Two sets of three resistive wave gauges (WG) are installed in the wave flume to measure the water surface elevation. The WGs were placed at two locations in the wave flume: before the start of the foreshore (WG1, WG2 and WG3 in Fig. 3) and near the toe of the structure (WG4, WG5 and WG6 in Fig. 3). The distances between the WGs were set for each test according to the recommendations by Mansard and Funke (1980). A separation into incident and reflected components of the water elevation at the two locations was made by the software WaveLab with the method of Zelt and Skjelbreia (1992). Moreover, two WGs were

installed near the wave paddle (AWA1 and AWA2 in Fig. 3) as part of the active wave absorption system. Gallach-Sánchez (2018) presents more details about the parameters of the active wave absorption system and the separation method of this research.

3.2. Test programme

The test programme of the experiments was designed to achieve the goal of improving the wave overtopping knowledge of steep low-crested structures. The various parameters considered in the test programme of each dataset are structural parameters (slope angle α [°], crest freeboard R_c [m]) and wave parameters at the toe of the structure (local water depth h [m], incident spectral wave height H_{m0} [m], incident peak wave period T_p [s] and incident wave period $T_{m-1,0}$ [s] defined by the ratio between the first negative moment and the zeroth moment of the spectrum m_{-1}/m_0 [−]).

Table 5 shows an overview of the ranges of parameters of the datasets UG13, UG14 and UG15, and the UG10 dataset for comparison. Fig. 5 shows the values of $\cot \alpha$ [−] compared to the relative crest freeboard R_c/H_{m0} [−] of each test of the datasets UG13, UG14 and UG15, while Fig. 6 shows the values of $\cot \alpha$ [−] compared to the relative wave height H_{m0}/h [−].

The three datasets UG13, UG14 and UG15 focus on steep low-crested structures, with slope angles $2.14 \geq \cot \alpha \geq 0$ and relative crest freeboards $2.92 \geq R_c/H_{m0} \geq 0$. The main differences between them are the relative water depth conditions of the tests. Nørgaard et al. (2014) use the relative wave height H_{m0}/h as a parameter to classify the relative water depth conditions. This classification distinguishes between relatively deep water conditions ($H_{m0}/h \leq 0.2$), transitional conditions ($0.2 < H_{m0}/h < 0.5$) and relatively shallow water conditions ($H_{m0}/h \geq 0.5$). The UG13 dataset feature mostly tests on relatively deep water conditions, although 21% of the tests are in transitional conditions. Also, 12% of this dataset is overlapping with the UG10 dataset. UG14 focus mainly on obtaining overtopping data for transitional conditions, with only 6% of the tests being performed for deep water conditions. UG15 extends the data towards the relatively shallow water conditions area, although also including tests for transitional conditions.

First order irregular waves were generated using a JONSWAP spectrum with a shape parameter of $\gamma = 3.3$, defined by the significant wave height H_s and peak wave period T_p. In each test, 1000 waves were analysed. The datasets are considered almost entirely in the non-breaking waves region, as the surf similarity parameter is $\xi_{m-1,0} > 2 - 3$ for nearly every test.

For most of the tests, the energy spectrum and wave period $T_{m-1,0}$ did not significantly change during the wave propagation from the wave paddle to the toe of the structure. This indicates that the UG13, UG14 and UG15 datasets cannot be included in the (very) shallow foreshores

Table 5
Overview of UG10, UG13, UG14 and UG15 datasets.

|	UG10	UG13	UG14	UG15
Number of tests [−]	366	307	435	197
Slope angle α [°]	20, 25, 30, 35, 40, 45, 50, 60, 70	25, 35, 45, 60, 75, 80, 85, 90	35, 45, 60, 70, 75, 80, 85, 90	35, 45, 60, 70, 75, 80, 85, 90
$\cot \alpha$ [−]	2.75, 2.14, 1.73, 1.43, 1.19, 1.00, 0.84, 0.58, 0.36	2.14, 1.43, 1.00, 0.58, 0.27, 0.18, 0.09, 0	1.43, 1.00, 0.58, 0.36, 0.27, 0.18, 0.09, 0	1.43, 1.00, 0.58, 0.36, 0.27, 0.18, 0.09, 0
Crest freeboard R_c [m]	0.020, 0.045, 0.070	0, 0.005, 0.01, 0.02, 0.045, 0.07	0, 0.02, 0.045, 0.076, 0.12, 0.2	0, 0.02, 0.045, 0.076, 0.12, 0.2
Incident spectral wave height at the toe H_{m0} [m]	0.023–0.19	0.018–0.16	0.061–0.225	0.107–0.22
Relative crest freeboard R_c/H_{m0} [−]	0.1–1.69	0–2.43	0–2.92	0.11–1.87
Target peak wave period T_p [s]	1.000–2.000	1.022–2.045	1.022, 1.534, 2.045	1.534, 2.045, 2.534
Relative wave height H_{m0}/h [−]	0.04–0.38	0.03–0.33	0.20, 0.30, 0.40, 0.50	0.30, 0.40, 0.50
Wave steepness $s_{m-1,0}$ [−]	0.016–0.056	0.014–0.047	0.012–0.062	0.01–0.05
Surf similarity parameter $\xi_{m-1,0}$ [−]	2–21.5	2.28–95	2.8–90	3.3–82
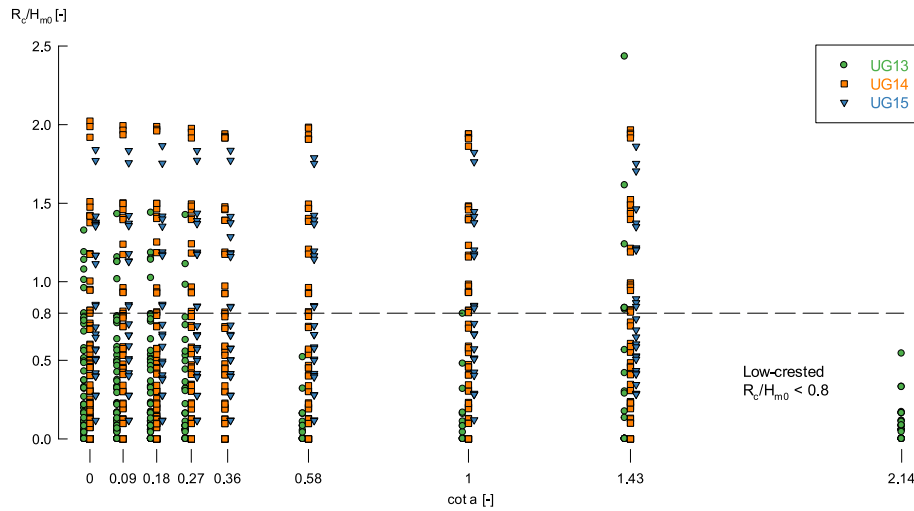
Fig. 5. Slope (cot α) and relative crest freeboard R_c/H_{m0} values tested on the UG13 (green circles), UG14 (orange squares) and UG15 (blue triangles) datasets, with indication of the low-crested structures range. The values on the cot α axis have been artificially shifted for clarity. (For interpretation of the references to colour in this figure legend, the reader is referred to the Web version of this article.)
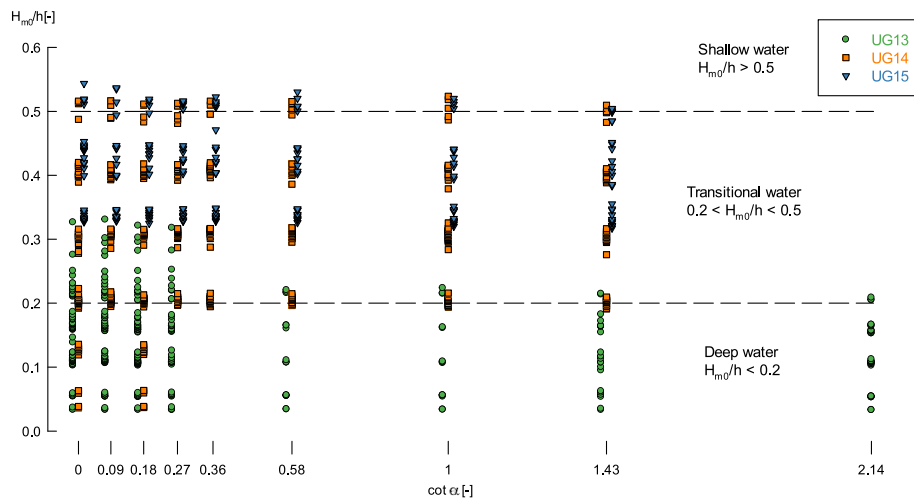

Fig. 6. Slope (cot α) and relative wave height H_{m0}/h values tested on the UG13 (green circles), UG14 (orange squares) and UG15 (blue triangles) datasets, with indication of the relative water depth ranges. The values on the cot α axis have been artificially shifted for clarity. (For interpretation of the references to colour in this figure legend, the reader is referred to the Web version of this article.)

research as for these foreshores the wave period $T_{m-1,0}$ heavily increases due to wave breaking (Altomare et al., 2016; Van Gent, 1999). Instead, in the relatively shallow water tests of these datasets the foreshore induces wave transformation (due to depth limitation) without breaking, which indicates the presence of an influencing foreshore as defined in the EurOtop (2018) manual. Moreover, the influence of the wave period $T_{m-1,0}$ on the average overtopping rates is negligible.

4. Data analysis of average overtopping rates for steep low-crested structures

In this section, the average overtopping data of the UG13, UG14 and UG15 datasets are compared to the existing average overtopping prediction formulae for steep low-crested structures referred in Section 2: Victor and Troch (2012a) (Eq. (2)) and Van der Meer and Bruce (2014) (Eq. (3)).

4.1. Comparison of data to existing prediction formulae

In general, both Eq. (2) and Eq. (3) predict correctly the average

overtopping rates for the range of steep low-crested structures. A complete comparison of the predictions with the data can be found in Gallach-Sánchez et al. (2018) for UG13, in Gallach-Sánchez et al. (2014) for UG14 and in Gallach-Sánchez et al. (2016) for UG15. To assess the accuracy of the prediction formulae, the root mean square error RMSE [−]:

$$RMSE = \sqrt{\frac{1}{N_{test}} \sum_{n=1}^{N_{test}} \left[\frac{q_{pred_n}}{\sqrt{gH_{m0}^3}} - \frac{q_{meas_n}}{\sqrt{gH_{m0}^3}} \right]^2} \quad (13)$$

and the relative mean square error rMSE [%] of the prediction are used:

$$rMSE = \frac{RMSE^2}{Var\left(\frac{q_{meas}}{\sqrt{gH_{m0}^3}}\right)} \cdot 100 \quad (14)$$

In Eq. (13) and Eq. (14), N_{test} [−] is the total number of data used to calculate the statistical parameter, q_{meas_n} [m³/s/m] is the absolute average overtopping measured for the test n, q_{pred_n} [m³/s/m] is the

Table 6

RMSE values (Eq. (13)) and rMSE (Eq. (14)) of the UG13, UG14 and UG15 datasets for different ranges of relative crest freeboard R_c/H_{m0} and slope angle α.

| Equation		Eq. 2		Eq. 3		Eq. 15	
Reference		Victor and Troch (2012a)		Van der Meer and Bruce (2014)		Present work	
Range	N_{test}	RMSE [−]	rMSE	RMSE [−]	rMSE	RMSE [−]	rMSE
All tests	938	0.0057	4.2%	0.0069	6.0%	0.0054	3.7%
UG13	307	0.0075	6.0%	0.0094	9.6%	0.0074	5.9%
UG14	434	0.0045	2.9%	0.0056	4.6%	0.0040	2.3%
UG15	197	0.0051	10.4%	0.0041	6.7%	0.0044	7.5%
Zero freeboard ($R_c = 0$)	140	0.0096	31.1%	0.0140	65.5%	0.0091	27.9%
$0 < R_c/H_{m0} < 0.05$	12	0.0078	36.4%	0.0090	48.6%	0.0076	34.6%
$0.05 < R_c/H_{m0} < 0.08$	27	0.0068	17.1%	0.0087	28.2%	0.0072	19.3%
$0.08 < R_c/H_{m0} < 0.11$	54	0.0065	23.1%	0.0078	33.0%	0.0066	24.2%
$0.11 < R_c/H_{m0} < 0.8$	453	0.0052	8.8%	0.0046	6.9%	0.0048	7.3%
$R_c/H_{m0} > 0.8$	252	0.0022	21.3%	0.0021	19.8%	0.0020	17.3%
Mild slopes	34	0.0119	49.2%	0.0123	52.7%	0.0118	48.9%
Steep slopes	354	0.0059	4.0%	0.0062	4.4%	0.0052	3.1%
Very steep slopes	387	0.0048	3.9%	0.0070	8.4%	0.0048	4.0%
Vertical structures	163	0.0054	6.8%	0.0064	9.5%	0.0049	5.5%
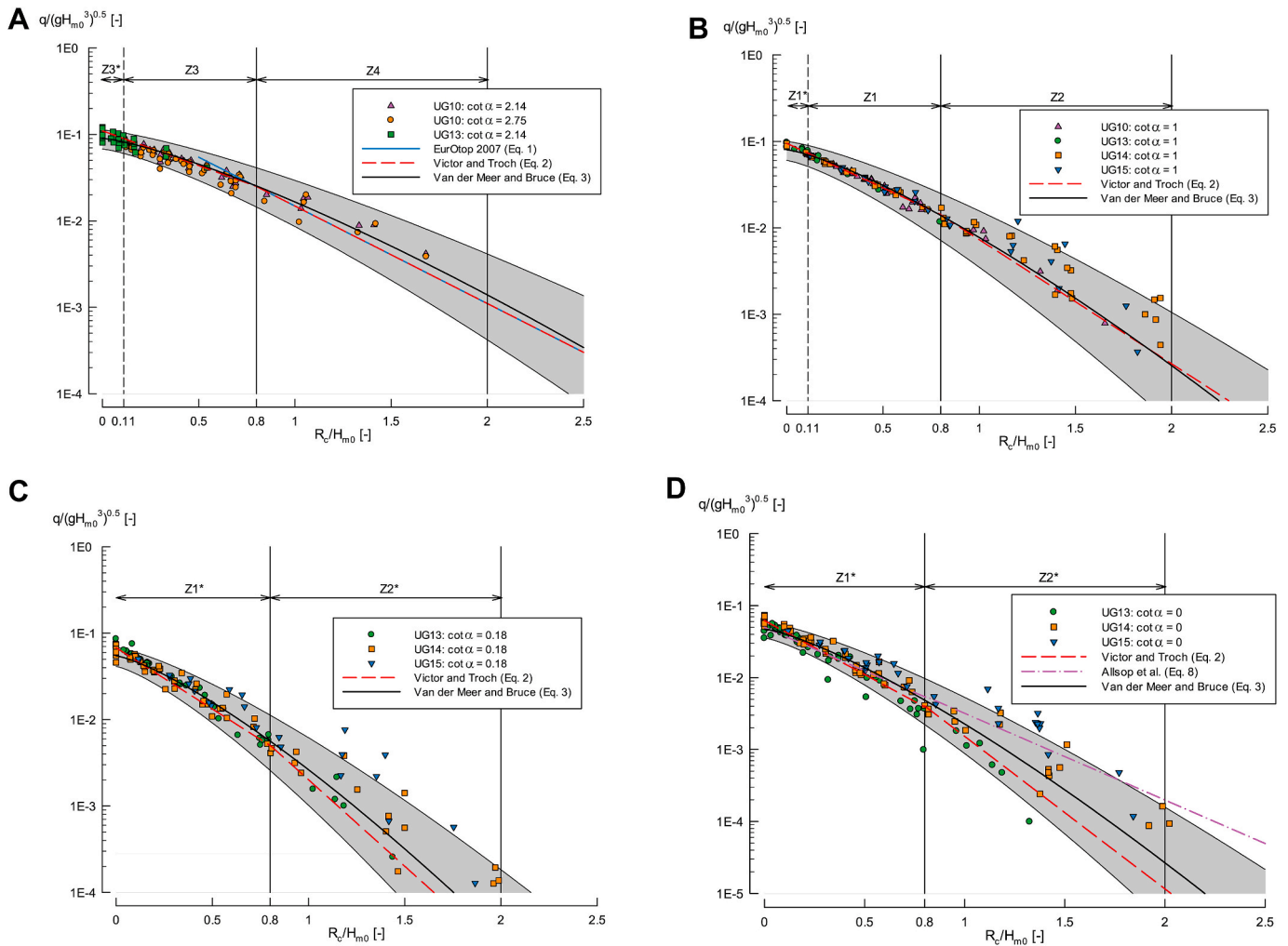
Fig. 7. Dimensionless average overtopping rate $q/\sqrt{gH_{m0}^3}$ versus relative crest freeboard R_c/H_{m0}, of the UG10, UG13, UG14 and UG15 datasets, compared to EurOtop (2007) (Eq. (1)), Victor and Troch (2012a) (Eq. (2)), Van der Meer and Bruce (2014) (Eq. (3)) with its 90% prediction band and Allsop et al. (1995) (Eq. (8)) for: mild slopes (upper left), steep slope $cot\,α = 1$ (upper right), very steep slope $cot\,α = 0.18$ (lower left) and vertical structures $cot\,α = 0$ (lower right).
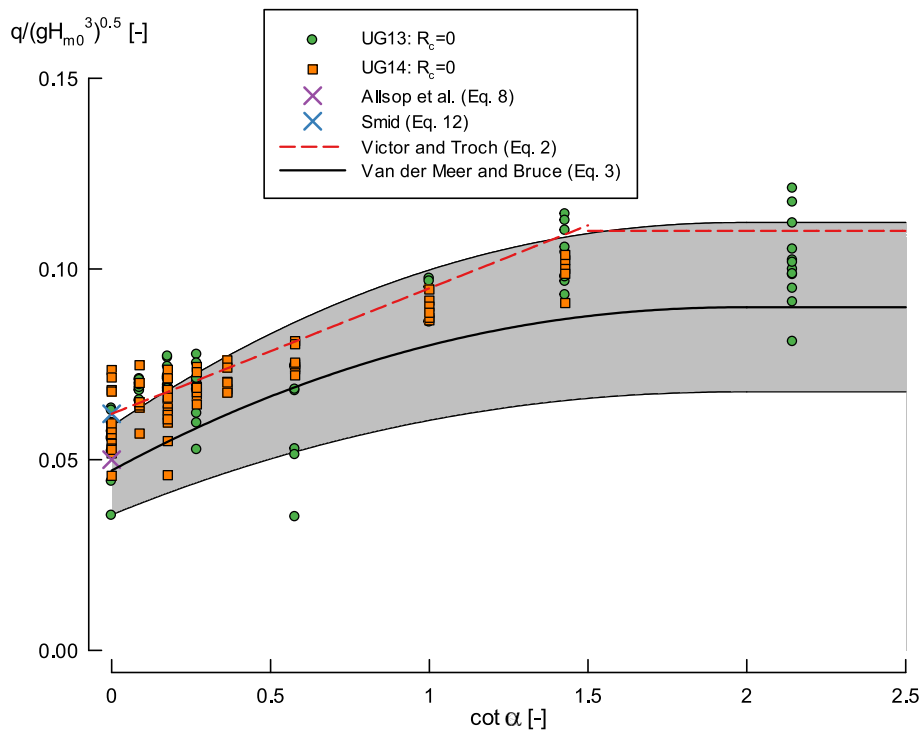
Fig. 8. Dimensionless average overtopping rate $q/\sqrt{gH_{m0}^3}$ versus slope angle $cot\,\alpha$ for the zero freeboard case ($R_c = 0$) of the UG13 and UG14 datasets compared to Allsop et al. (1995) (Eq. (8)), Smid (2001) (Eq. (12)), Victor and Troch (2012a) (Eq. (2)) and Van der Meer and Bruce (2014) (Eq. (3)) with its 90% prediction band.

absolute average overtopping predicted for the test n, and $Var\left(\frac{q_{meas}}{\sqrt{gH_{m0}^3}}\right)$ [−] is the variance of the dimensionless average overtopping measured for a specific set of data.

The RMSE estimates the accuracy of a prediction within the same set of data. A lower RMSE means a more accurate prediction than a higher RMSE value. The rMSE indicates whether the prediction can model the natural variability of the data. The value of the rMSE is the percentage of the variance of the measured data not explained by the prediction. A lower rMSE means that the prediction is able to model correctly the natural variability of the data in a given set.

Table 6 shows the RMSE values (Eq. (13)) and rMSE values (Eq. (14)) of the overtopping predictions by Victor and Troch (2012a) (Eq. (2)) and Van der Meer and Bruce (2014) (Eq.(3)). This table also includes the new prediction resulting from this paper (Eq. (15)), which will be discussed later on in Section 5.3. The RMSE and rMSE are shown for the UG13, UG14 and UG15 datasets and the combination of the three datasets for different ranges of the slope angle α (Table 1), and relative crest freeboard R_c/H_{m0} (Table 2). The very small relative crest freeboard range is further subdivided for deeper insights into the accuracy of the predictions.

In general, Eq. (2) shows smaller or similar RMSE values than Eq. (3) for all the data (except for the dataset UG15). The hypothesis is that Eq. (2) describes better the shape of the relative average overtopping data than Eq. (3), especially for smaller relative crest freeboards (for which the UG15 dataset has no data). For the zero freeboard case ($R_c = 0$), the RMSE of Eq. (2) is 31% smaller than the RMSE of Eq. (3). For $R_c/H_{m0} > 0.11$ (small and large relative crest freeboards), the two predictions have similar RMSE values, with Eq. (3) performing slightly better than Eq. (2). The RMSE values are increasingly smaller for larger relative crest freeboards, indicating that Eq. (2) and Eq. (3) were fitted through overtopping data in the range of large relative crest freeboards. These results confirm the previously raised hypothesis.

The RMSE values for mild slopes in the two predictions are larger than for steep, very steep slopes and vertical structures. This can be due to the relatively small number of tests in the range of mild slopes ($N_{test} = 34$) compared to the number of tests in the other ranges ($N_{test} = 354, 387$ and 163, respectively). Eq. (2) shows consistently smaller RMSE values than Eq. (3) for all the slope angle ranges.

The rMSE values indicate that the natural variability of the overtopping data is in general well explained by Eq. (2) and Eq. (3) for the three datasets, with values lower or around 10%. However, for the zero freeboard case ($R_c = 0$) and very small relative crest freeboards ($0 < R_c/H_{m0} \leq 0.11$), the variability of the data not explained by the predictions has values higher than 30%, reaching up to 65.5% in the case of $R_c = 0$ for Eq. (3). The rMSE values for these ranges are higher than for larger relative crest freeboards.

For UG13 and UG14, the prediction for very small and zero relative freeboards ($0 \leq R_c/H_{m0} \leq 0.11$) by Eq. (2) is more accurate than the prediction by Eq. (3). As Eq. (2) divides the full range of R_c/H_{m0} in two zones (see Table 3), the shape of the prediction adapts better to the shape of the data than Eq. (3), which is dominated by the coefficient $c_{V\&B} = 1.3$ causing an underprediction of the overtopping for very small and zero relative freeboards. For small ($0.11 < R_c/H_{m0} < 0.8$) and large ($R_c/H_{m0} > 0.8$) relative crest freeboards, Eq. (3) has a similar accuracy to Eq. (2) on the three datasets, as both prediction formulae were fitted through the UG10 dataset, which contained overtopping data in this range.

Fig. 7 shows the U10, UG13, UG14 and UG15 data for mild slopes (upper left panel), the steep slope $cot\,\alpha = 1$ (upper right) the very steep slope $cot\,\alpha = 0.18$ (lower left) and vertical structures $cot\,\alpha = 0$ (lower right). These data are compared to the prediction by Victor and Troch (2012a) (Eq. (2), red dashed line) and Van der Meer and Bruce (2014) (Eq. (3), black solid line) with its 90% prediction band. The EurOtop (2007) manual prediction (Eq. (1), blue solid line) is also compared for mild slopes, and the Allsop et al. (1995) (Eq. (8), purple dash dotted line) for vertical structures.

The new zones Z1* ($0.27 \geq cot\,\alpha > 0$, $0.8 > R_c/H_{m0} \geq 0$), Z2* ($0.27 \geq cot\,\alpha > 0$, $2 > R_c/H_{m0} \geq 0.8$) and Z3* ($2.75 \geq cot\,\alpha > 1.5$, $R_c/H_{m0} < 0.11$) are defined based on the data from the UG13, UG14 and

Table 7
Percentage of UG13, UG14 and UG15 tests outside the 90% prediction band of Eq. (3) for various ranges of relative crest freeboard R_c/H_{m0}.

Percentage of tests outside 90% prediction band of Eq. (3)			
Range	UG13	UG14	UG15
All tests	15.6	10.1	23.4
Zero freeboard ($R_c = 0$)	45.2	25.4	N/A
$0 < R_c/H_{m0} < 0.05$	16.7	N/A	N/A
$0.05 < R_c/H_{m0} < 0.08$	9.5	0	N/A
$0.08 < R_c/H_{m0} < 0.11$	0	11.1	N/A
$0.11 < R_c/H_{m0} < 0.8$	6.5	0.5	10.0
$R_c/H_{m0} > 0.8$	7.7	17.3	40.2

UG15 datasets that extend the original Z1, Z2, Z3 and Z4 zones (see Table 3).

For mild slopes, the accuracy of the three predictions is good. However, in the zone Z3* (very small relative freeboards), Eq. (3) is slightly underpredicting the dimensionless average overtopping rate (with a RMSE = 0.0137) probably due to the fact that the prediction has not been fitted through overtopping data on that range. For large relative freeboards the prediction by Eq. (3) is very similar to the prediction obtained by Eq. (1), while Eq. (2) matches the prediction by Eq. (1) as explained in Section 2.2.1.

For steep, very steep and vertical structures, the accuracy of Eq. (2) and Eq. (3) is good with some exceptions. In the zone Z1* (small relative crest freeboards of very steep slopes and vertical structures), the trend of the data for relative crest freeboards $R_c/H_{m0} \leq 0.25$ diverges from the prediction of Eq. (3), resulting in an underprediction of the overtopping values. This is in agreement with the underprediction for very small and zero relative crest freeboards shown in the overview of RMSE values (Table 6). Eq. (2) adapts better to the shape of the data in the zone Z1* for very small and zero freeboards thanks to its bilinear shape in a semilogarithmic plot. In the zone Z2* (large relative freeboards of very steep slopes and vertical structures), both predictions are underestimating the overtopping rates of the UG14 and UG15 datasets.

For vertical structures, Allsop et al. (1995) (Eq. (8)) is predicting the tests of the UG14 and UG15 datasets with a higher accuracy than Eq. (2) and Eq. (3). These datasets feature tests with relatively shallow and transitional water conditions, which can be considered as having an influencing foreshore (see Section 3.2). This confirms that Eq. (8) is suitable to predict the average overtopping rates of vertical structures with influencing foreshores and non-breaking conditions as suggested in the EurOtop (2018) manual.

For very small and zero relative crest freeboards, a consistent underprediction of the overtopping values for both formulae is seen across all the datasets for all the slopes considered, from mild to vertical. This is also confirmed by Fig. 8 which shows the UG13 and UG14 zero freeboard ($R_c = 0$) data compared to the prediction by Victor and Troch (2012a) (Eq. (2), red dashed line) and Van der Meer and Bruce (2014) (Eq. (3), black solid line) with its 90% prediction band. For vertical structures, also the predictions by Allsop et al. (1995) (Eq. (8), purple cross) and Smid (2001) (Eq. (12), blue cross) are shown.

For these zero freeboard conditions, Eq. (2) is predicting the overtopping rates with a higher accuracy than Eq. (3), which underpredicts almost all the overtopping values. This confirms the RMSE and rMSE values in Table 6. For vertical structures with zero freeboard conditions, Eq. (12) is correctly predicting the overtopping rates (with the same prediction as Eq. (2)), while Eq. (8) is underpredicting the results.

Moreover, as shown in Table 7, for tests with zero freeboard ($R_c = 0$) 45.2% of the UG13 dataset (from a total of 73 tests) and 25.4% of the UG14 (from a total of 67 tests) are predicted outside the 90% prediction band of Eq. (3). By definition, only 10% of the tests should be predicted outside the 90% prediction band (considering a sufficiently large dataset). Also for $0 < R_c/H_{m0} < 0.05$ (inside the range of very small

freeboards defined in Table 2), 16.7% of the UG13 tests are predicted outside the 90% prediction band. For small ($0.11 < R_c/H_{m0} < 0.8$) and large ($R_c/H_{m0} > 0.8$) relative crest freeboards, the percentage is lower than (or around) 10% for the UG13, UG14 and UG15 datasets.

For large relative crest freeboards ($R_c/H_{m0} > 0.8$), 17.3% of the UG14 tests in this range and 40.2% of the UG15 tests in this range are outside the 90% prediction band of Eq. (3). However, for the UG13 dataset, only 7.7% of the tests in this range are outside the band. As the UG14 and UG15 datasets feature tests on relatively transitional and shallow water conditions ($H_{m0}/h \geq 0.2$), the conclusion is that these datasets are underpredicted for large relative freeboards by the considered formulae due to shallow water effects.

4.2. Discussion

Between Victor and Troch (2012a) (Eq. (2) and Table 3) and Van der Meer and Bruce (2014) (Eq. (3)) predictions, there is a special interest in the latter prediction, as it is recommended in the EurOtop (2018) manual as the reference prediction for very steep slopes to vertical walls, including those with very small and zero freeboard. However, the prediction formulae by Victor and Troch (2012a) are in general more accurate (i.e., smaller RMSE values for the same set of data) in predicting the overtopping values of the UG13, UG14 and UG15 dataset than the Van der Meer and Bruce (2014) formula.

Nevertheless, none of the predictions where validated explicitly by data for very steep slopes to vertical structures, and very small to zero freeboards (i.e., steep low-crested structures). UG13, UG14 and UG15 can be used to check the accuracy of the prediction in this range, which previously was a knowledge gap in the literature. For these conditions, the new zones Z1* ($0.27 \geq \cot \alpha > 0$, $0.8 > R_c/H_{m0} \geq 0$) and Z2* ($0.27 \geq \cot \alpha > 0$, $2 > R_c/H_{m0} \geq 0.8$) are defined with the extension data of the new datasets. Eq. (3) has a good accuracy for mild slopes and steep slopes, while for very steep slopes (Fig. 7) and vertical structures the trend of the data is slightly different than the prediction, causing a small overprediction for relative crest freeboards $R_c/H_{m0} \geq 0.25$ and a small underprediction for $R_c/H_{m0} < 0.25$ (Gallach-Sánchez et al., 2018).

For very small and zero relative crest freeboards ($0.11 \geq R_c/H_{m0} \geq 0$) there is a consistent underprediction across all the slope angles by Eq. (3). This is confirmed graphically by Fig. 8, by the RMSE values for various ranges of relative crest freeboards (Table 6) and by the large percentage of UG13 and UG14 data for zero freeboard outside the 90% prediction band of the prediction (Table 7).

The accuracy of the prediction by Van der Meer and Bruce (2014) can be improved by adding the UG13, UG14 and UG15 datasets to the previous UG10 dataset and CLASH data and refitting the a, b and c coefficients in Eq. (3). This is possible through the complete range of slope angles ($\cot \alpha \geq 0$) and relative crest freeboards ($R_c/H_{m0} \geq 0$). The methodology used in the refitting of the coefficients will be formulated in detail in the following section.

5. New average overtopping prediction formula for steep low-crested structures

As stated in Section 4.2, it is possible to propose a new average overtopping prediction formula that improves the accuracy of the existing ones by including the new overtopping datasets UG13, UG14 and UG15 in the fitting of the prediction. In particular, a higher prediction accuracy is wanted for:

i. Vertical structures ($\cot \alpha = 0$);
ii. Very steep slopes ($0.27 \geq \cot \alpha > 0$); and
iii. Very small and zero relative freeboards ($0.11 > R_c/H_{m0} \geq 0$).

The new prediction should maintain the accuracy achieved by Victor and Troch (2012a) and Van der Meer and Bruce (2014) for steep slopes ($2 > \cot \alpha > 0.27$) and mild slopes ($\cot \alpha \geq 2$) with small

$(0.8 > R_c/H_{m0} \geq 0.11)$ and large $(R_c/H_{m0} \geq 0.8)$ relative crest freeboards.

5.1. Selection of overtopping data to fit the new prediction

The overtopping data considered for the fitting of the new prediction belong to the UG10, UG13, UG14 and UG15 datasets, the CLASH database and overtopping data for vertical walls reported in the EurOtop (2018) manual. However, not all the tests are suitable to be included in the fitting due to various reasons. To have a consistent overtopping dataset to fit the new prediction, only tests with similar setups and wave conditions should be chosen.

The criteria and the reasons to select tests to be included in the fitting of the new prediction are:

1. Foreshore at the toe of the structure milder than 1:100, to avoid depth-limited wave breaking and to match the mild foreshores of all the datasets obtained at Ghent University (see Section 3.1).
2. No complex cross sections, as the presence of a toe or a berm influences the overtopping rates. The only exception is for composite vertical structures without influencing foreshore, as the EurOtop (2018) manual decision chart (Figure 7.2 of the manual) states that in this case the overtopping is not influenced by the presence of a toe or a berm.
3. Smooth and impermeable structures ($\gamma_f = 1$), as the effect of rough slopes and permeable structures should be excluded for the analysis of the overtopping at this stage.
4. Perpendicular wave attack ($\beta = 0°$, $\gamma_\beta = 1$), to exclude from the analysis the effect of oblique wave attack on the overtopping rates.
5. Slope angle $\cot \alpha \leq 4$, as the purpose is to update the steep low-crested overtopping prediction formula.
6. Tests with non-breaking wave conditions, as the prediction formula to update is for non-breaking conditions. Tests with a surf similarity parameter $\xi_{m-1,0} < 2$, and tests which are described by the breaking prediction formula by Van der Meer and Bruce (2014) are excluded from the fit.
7. Relatively deep water conditions ($H_{m0}/h < 0.2$) and transitional conditions ($0.2 < H_{m0}/h < 0.4$). As discussed in Section 4.1, relatively shallow water conditions have an effect on the overtopping rates. Therefore, tests with $H_{m0}/h > 0.4$ are excluded from the fit. The limit value of $H_{m0}/h = 0.4$ is taken to match the values of H_{m0}/h tested in the UG10 dataset.
8. No tests with zero overtopping or with average overtopping $q < 1 \cdot 10^{-6}$ m³/s/m, following the approach of the authors of several neural networks (Van Gent et al., 2007; Verhaeghe et al., 2008; Zanuttigh et al., 2016).

By applying these criteria, a total of 1410 tests (called from now on the fitting dataset) of the following datasets fitted the new average overtopping prediction formula:

- UG10 dataset: 311 tests.
- UG13 dataset: 297 tests.
- UG14 dataset: 322 tests.
- UG15 dataset: 91 tests.
- CLASH: 322 tests. Subsets (most of them partially): 028, 102, 103, 106, 107, 113, 218, 220, 221, 222, 226, 228, 229, 315, 351, 380, 402, 510, 703, 914. Subsets with a Reliability Factor RF = 4 were analysed and discarded only if the average overtopping rates were not in line with the expected values. Three tests from subset 028 and 55 tests from subset 107 are included in the fitting dataset with a RF = 4.
- Tests reported in Figure 7.7 of the EurOtop (2018) manual on vertical structures without influencing foreshore: 67 tests (obtained in a personal communication with Prof. Van der Meer).

5.2. Fit of the coefficients

The new average overtopping prediction formula for non-breaking conditions is the Weibull-type shown in Eq. (15). The resulting fitted expressions of the coefficients a, b and c are shown in Eqs. (16)–(18), respectively:

$$\frac{q}{\sqrt{gH_{m0}^3}} = a \cdot \exp\left(-\left(b \frac{R_c}{H_{m0} \cdot \gamma_f \cdot \gamma_\beta}\right)^c\right) \qquad (15)$$

with the following expressions for the coefficients a, b and c:

$$a = 0.109 - 0.035 \cdot (1.5 - \cot \alpha) \text{ for } \cot \alpha \leq 1.5$$
$$\text{and } a = 0.109 \text{ for } \cot \alpha > 1.5 \qquad (16)$$

$$b = 2 + 0.56(1.5 - \cot \alpha)^{1.3} \quad \text{for } \cot \alpha \leq 1.5$$
$$\text{and } b = 2 \text{ for } \cot \alpha > 1.5 \qquad (17)$$

$$c = 1.1 \qquad (18)$$

The uncertainty related to the a coefficient is defined by a standard error of the estimate $\sigma_{est}(a) = 0.01$ and the uncertainty related to the b coefficient is defined by a standard error of the estimate $\sigma_{est}(b) = 0.4$ (see Section 5.2.4). The range of application of the formula is for slope angles $0 \leq \cot \alpha \leq 4$ and relative crest freeboards $R_c/H_{m0} \geq 0$. The coefficients a, b and c (Eqs. (16)–(18)) represent the mean value approach of the prediction. For design purposes and safety assessments, the average overtopping prediction should be increased by one standard deviation (EurOtop, 2018).

Eq. (15) includes the roughness influence factor γ_f and the oblique wave attack influence factor γ_β in the prediction. The various γ_f and γ_β
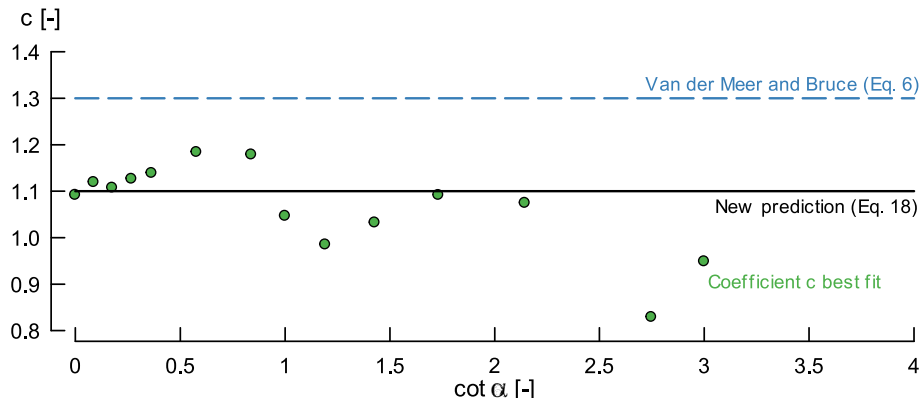

Fig. 9. Best fit of the c coefficient per slope angle and new value $c = 1.1$ compared to Van der Meer and Bruce (2014) ($c = 1.3$).
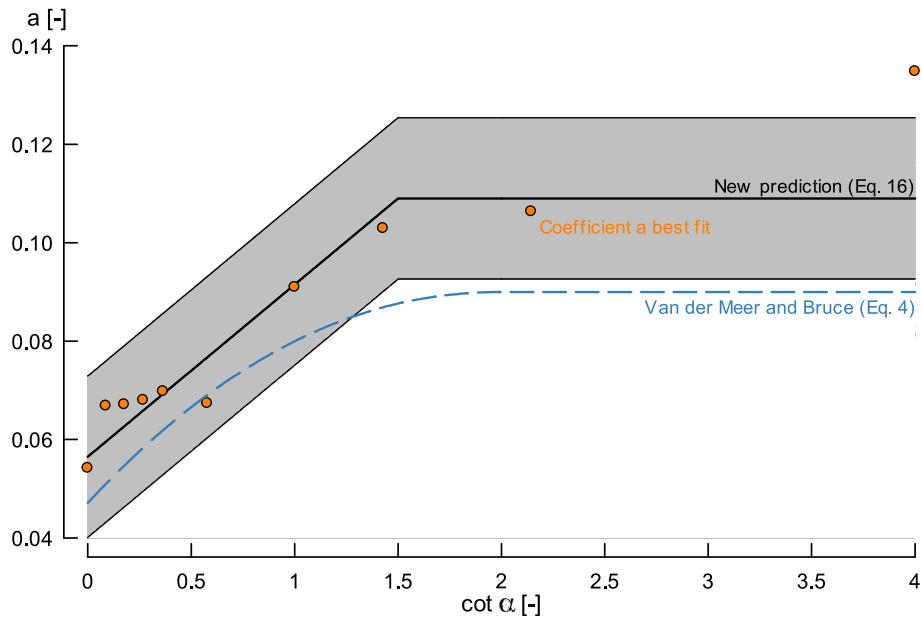
Fig. 10. Best fit of the *a* coefficient (Eq. (16) with its 90% prediction band) for tests with $R_c/H_{m0} = 0$ (only) compared to Van der Meer and Bruce (2014) (Eq. (4)).

expressions published in literature (e.g., in the EurOtop (2018) manual) are fitted through Eq. (1) with a $c = 1.0$ and therefore it is mathematically incorrect to use them in Eq. (15). New γ_f and γ_β expressions should be obtained by refitting through Eq. (15) existing average overtopping data for rubble mound structures and under oblique wave attack. It is possible to estimate the prediction error made when using the published γ_f and γ_β coefficients fitted for Eq. (1) in Eq. (15). For a relative crest freeboard $R_c/H_{m0} = 0.5$ (the minimum relative crest freeboard applicable for Eq. (1)), the new prediction results in an overtopping rate a 26% lower for $\gamma_f = 1$ and a 9% lower for $\gamma_f = 0.4$ than Eq. (1). These underpredictions are within the 90% prediction band of Eq. (15) (see Section 5.2.4), which has a factor 2.8 bandwidth. For large values of the relative crest freeboard R_c/H_{m0}, Eq. (1) and Eq. (15) have very similar overtopping predictions and therefore the error made when using the existing γ_f and γ_β factors is negligible.

A nonlinear regression is performed to find the best fit of the *a*, *b* and *c* coefficients per slope angle by minimizing the residual sum of squares (RSS [−], as shown in Eq. (19)). The RSS has a similar formulation to RMSE (Eq. (13)):

$$RSS = \sum_{n=1}^{N_{test}} \left[\frac{q_{pred_n}}{\sqrt{gH_{m0}^3}} - \frac{q_{meas_n}}{\sqrt{gH_{m0}^3}} \right]^2 \tag{19}$$

5.2.1. Coefficient c

The data used to fit the new prediction (Fig. 9) do not show a dependence of *c* on the slope angle, therefore, we propose to have a constant value for the *c* coefficient. The best fit of the new *c* coefficient is found to be $c = 1.1$.

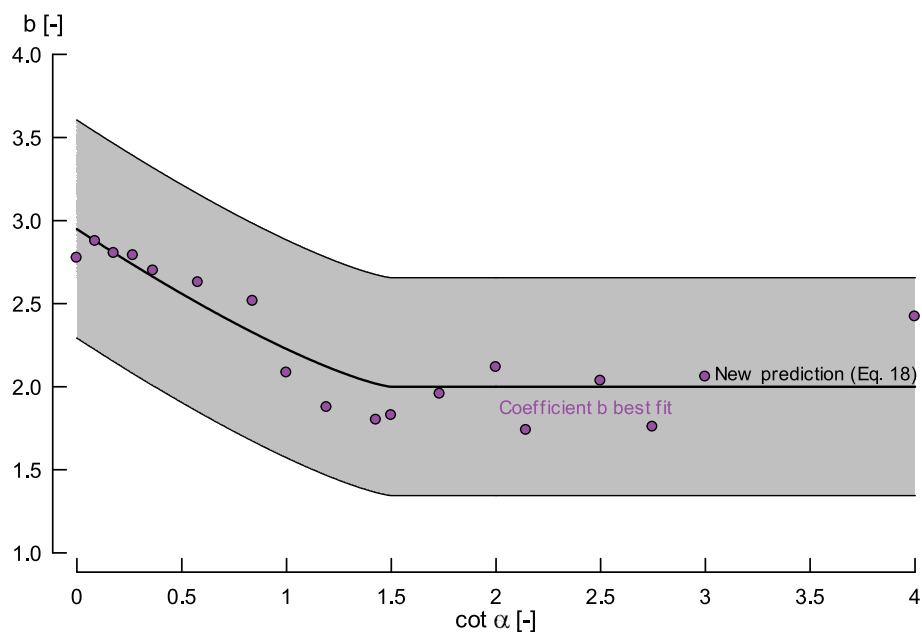The data per slope angle (Fig. 9) show that $c = 1.3$ is overestimating

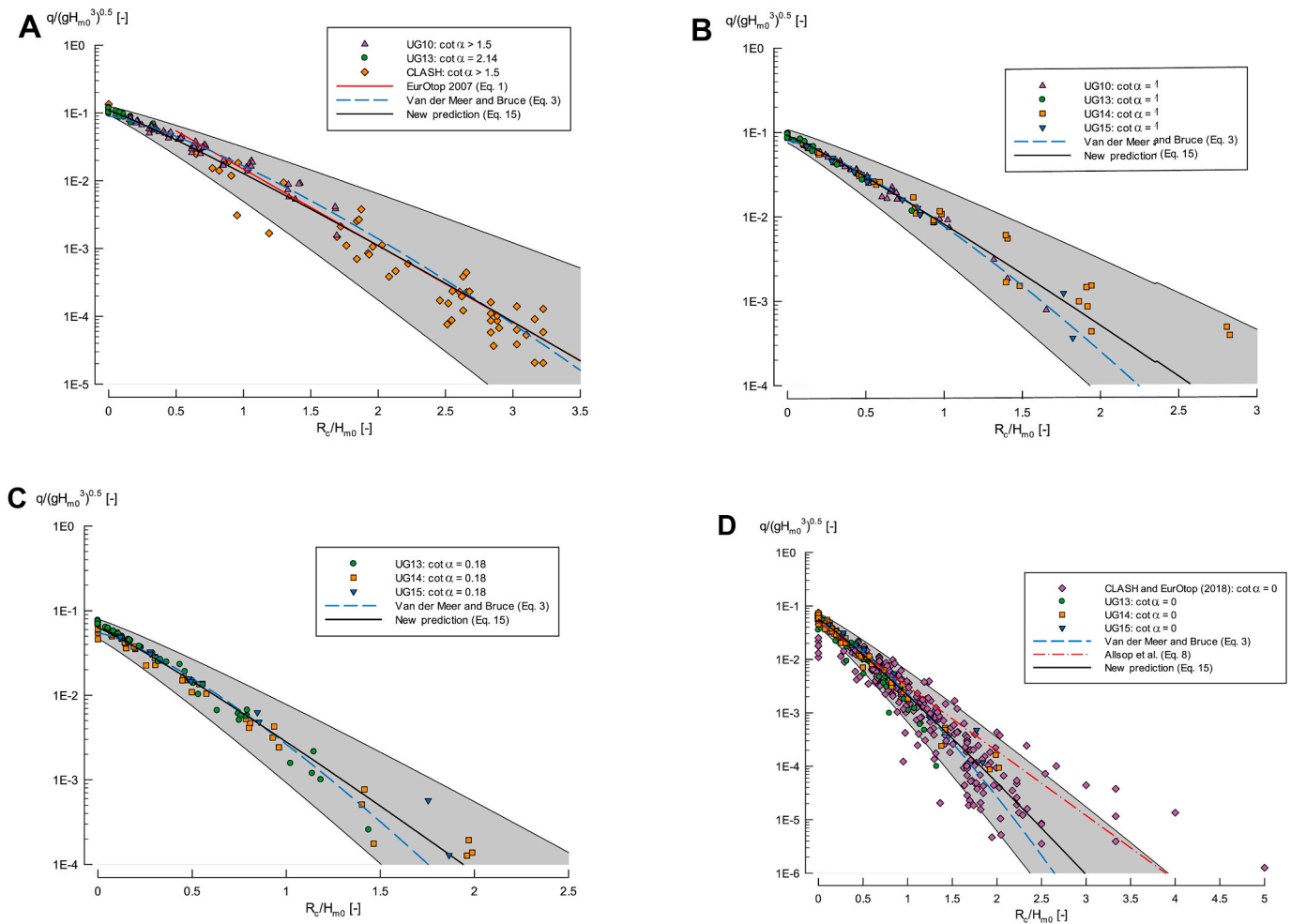**Fig. 11.** Best fit of the *b* coefficient (Eq. (17) with its 90% prediction band).

Fig. 12. Dimensionless average overtopping rate $q/\sqrt{gH_{m0}^3}$ versus relative crest freeboard R_c/H_{m0} of the fitting dataset compared to EurOtop (2007) (Eq. (1)), Van der Meer and Bruce (2014) (Eq. (3)), Allsop et al. (1995) (Eq. (8)) and the new prediction (Eq. (15)) with its 90% prediction band for: mild slopes (upper left), steep slope $\cot\alpha = 1$ (upper right), very steep slope $\cot\alpha = 0.18$ (lower left) and vertical structures $\cot\alpha = 0$ (lower right).

the best c for all the slope angles considered. As it is explained in Van der Meer et al. (2013), the value $c = 1.3$ is both valid for breaking and non-breaking conditions although it is not the best fit for the non-breaking tests.

The obtained values of c for each slope angle (Fig. 9) also suggest that the shape of overtopping data for the complete range of relative crest freeboards is closer to a line in a semilogarithmic plot than estimated by Van der Meer et al. (2013) and Van der Meer and Bruce (2014). This inaccurate estimation is maybe due to lack of a significant number of overtopping data available for zero and very small freeboards at the time of both publications. This closer to linear shape was already observed in the data when comparing UG13, UG14 and UG15 with Eq. (3) (see Section 4.1). The value of $c = 1.1$ yields a prediction trend close to a straight line in a semilogarithmic plot, matching better the shape of the data.

5.2.2. Coefficient a

The best fit of the a coefficients (Fig. 10) is found among the zero freeboard data ($R_c = 0$) to assure the most accurate prediction for these conditions, resulting in Eq. (16). The a coefficients show a dependence on the slope angle, although only for values $\cot\alpha < 1.5$. This limit differs from Van der Meer and Bruce (2014) who found a limit on $\cot\alpha = 2$ but is the same value found by Victor and Troch (2012a). The new a coefficient has a similar expression to Eq. (4) although with a linear shape, reaching a constant value at $\cot\alpha = 1.5$. The resulting expression for a results in larger values for the new prediction than for Eq. (4).

5.2.3. Coefficient b

A linearisation is applied to the fitting dataset by calculating the natural logarithm of both sides of Eq. (16). On this step, the values of c and a are fixed according to $c = 1.1$ and Eq. (16), respectively. The best power law with the same shape as Eq. (5) is calculated through the linearised b values per slope angle for all values of R_c/H_{m0}, resulting in Eq. (17) (Fig. 11). Compared to Eq. (5), Eq. (17) does not have a constant maximum value of b as the data show increasing values of b at this range of slopes. The influence of slope angle α is found to be until $\cot\alpha = 1.5$, matching Victor and Troch (2012a) and diverging from Van der Meer and Bruce (2014), as was the case for the coefficient a.

A direct comparison of the b coefficient values between the new prediction (Eq. (17)) and the Van der Meer and Bruce (2014) prediction (Eq. (5)) is not possible as the values of b are affected by the value of the coefficient c, which is different for both predictions.

5.2.4. Uncertainty of the new prediction

The EurOtop (2018) manual describes the uncertainty of the Van der Meer and Bruce (2014) prediction by a coefficient of variation $\sigma' = \sigma/\mu$ of $a_{V\&B}$ and $b_{V\&B}$ (where σ is the standard deviation and μ the average value of the coefficient for a specific slope angle). However, for the new prediction the uncertainty is described by a single value of the standard error of the estimate σ_{est} for the coefficients a and b. To suggest a coefficient of variation σ' instead of the standard error of the estimate σ_{est} implies that the uncertainty is larger for larger values of the considered
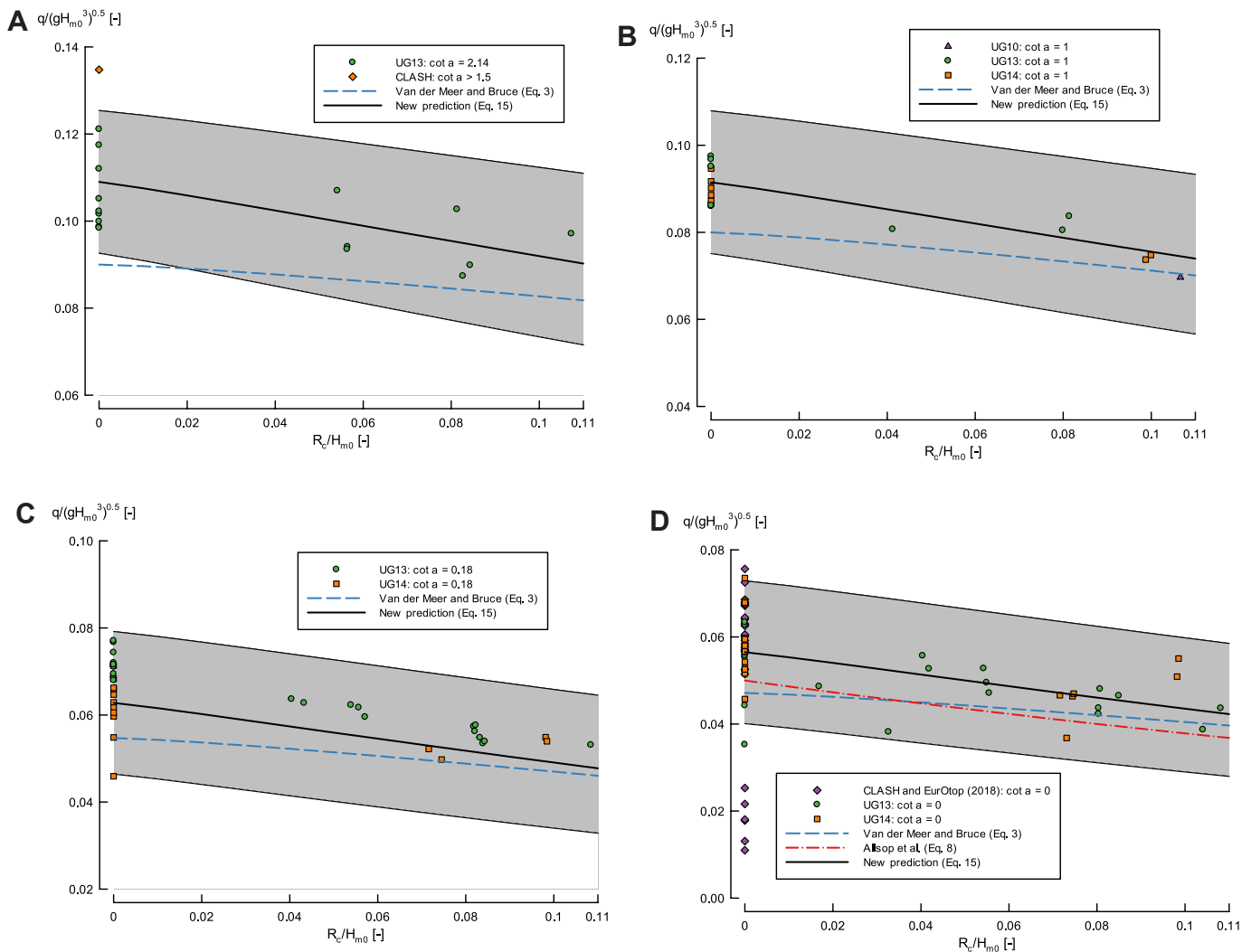
Fig. 13. Dimensionless average overtopping rate $q/\sqrt{gH_{m0}^3}$ (linear scale) versus relative crest freeboard R_c/H_{m0} of the fitting dataset for very small and zero relative freeboards ($0 \leq R_c/H_{m0} < 0.11$), Van der Meer and Bruce (2014) (Eq. (3)), Allsop et al. (1995) (Eq. (8)) and the new prediction (Eq. (15)) with its 90% prediction band for: mild slopes (upper left), steep slope $\cot\alpha = 1$ (upper right), very steep slope $\cot\alpha = 0.18$ (lower left) and vertical structures $\cot\alpha = 0$ (lower right).

coefficient, whereas the data show no influence of the slope angle α on the uncertainty of the prediction.

The uncertainty of the a coefficient (Eq. (16)) is obtained by calculating the standard error of the estimate a of all the $R_c = 0$ tests, which results in $\sigma_{est}(a) = 0.01$. The 90% prediction band of a is calculated by $a \pm 1.64 \cdot \sigma_{est}(a)$, assuming that a is a normally distributed stochastic parameter.

The uncertainty of the b coefficient (Eq. (17)) is defined by a standard error of the estimate $\sigma_{est}(b) = 0.4$. One result of the linearisation process described in Section 5.2.3 (in which the coefficients a and c are fixed before obtaining the b coefficient) is that for tests with small relative crest freeboards, the uncertainty of the measured b coefficients is artificially increased and it is not representative of larger relative crest freeboards. This is due to the differences between the measured a coefficients of each test and the final expression of a (Eq. (16)). After a sensitivity analysis, the uncertainty of b is stable for relative crest freeboards $R_c/H_{m0} > 0.45$ at a value $\sigma_{est}(b) = 0.4$. The 90% prediction band of b is calculated by $b \pm 1.64 \cdot \sigma_{est}(b)$, assuming that b is a normally distributed stochastic parameter.

5.3. Comparison of predictions and discussion

The comparison between Eq. (3) and Eq. (15) was seen in Fig. 2. Eq.

(15) gives a larger prediction than Eq. (3) for zero freeboards ($R_c = 0$) as a result of a being larger than $a_{V\&B}$ for the complete range of slope angles. The higher predicted value for $R_c = 0$ solves the prediction inaccuracy by Eq. (3) for this case stated in Section 4.1.

For larger relative freeboards, both predictions are similar in the case of mild slopes ($\cot\alpha \geq 2$), with the EurOtop (2007) prediction (Eq. (1)) applicable in this range and predicting accurately the overtopping rates for $R_c/H_{m0} > 1$ (Gallach-Sánchez et al., 2018). For steeper slopes, the new prediction yields larger overtopping rates than Eq. (3) due to the smaller coefficient $c = 1.1$ of the updated prediction as it adapts better to the shape of the data.

Fig. 12 shows the new prediction compared to the fitting dataset for mild slopes ($\cot\alpha > 1.5$), the steep slope $\cot\alpha = 1$, the very steep slope $\cot\alpha = 0.18$ and vertical structures ($\cot\alpha = 0$). In general, the new prediction improves the accuracy of Eq. (3). For vertical structures, whereas Eq. (3) is recommended in the EurOtop (2018) manual to be used only to predict overtopping with no influencing foreshores, Eq. (15) takes the scatter of the data that accounts for shallower water conditions—a possible presence of an influencing foreshore—in the uncertainty determination. Therefore, Eq. (15) is applicable for both influencing and no influencing foreshores in the case of vertical structures, and for no influencing foreshores in the case of vertical composite structures.
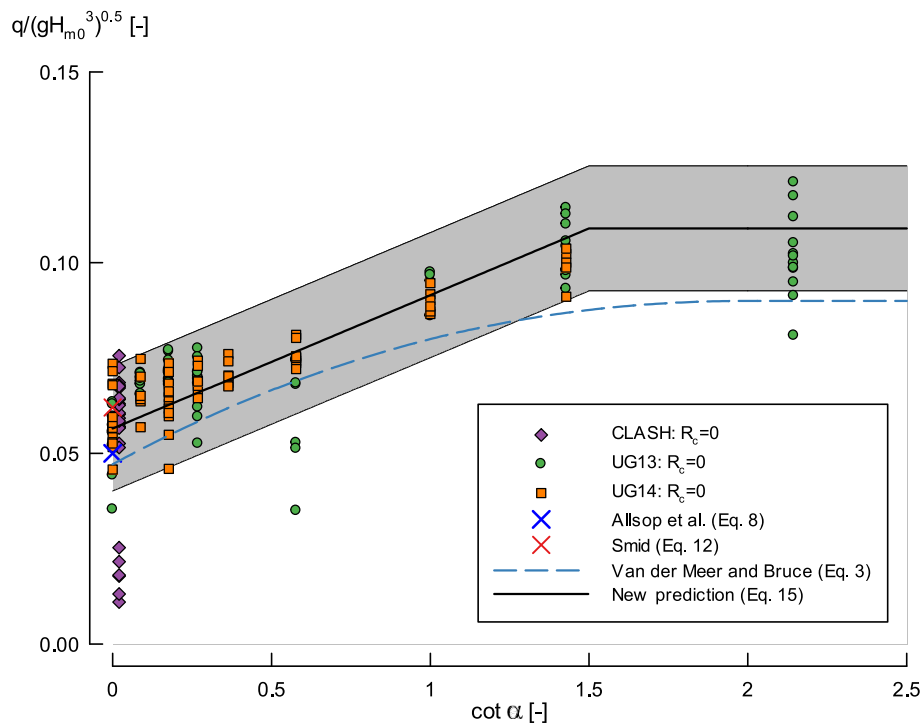
Fig. 14. Zero freeboard ($R_c = 0$) tests of the fitting dataset compared to Allsop et al. (1995) (Eq. (8)), Smid (2001) (Eq. (12)), Van der Meer and Bruce (2014) (Eq. (3)) and the new prediction (Eq. (15)) with its 90% prediction band. CLASH data for $cot\ \alpha = 0$ have been artificially shifted to the right for clarity.

The RMSE and rMSE values of Eq. (15) for the UG13, UG14 and UG15 datasets are shown in Table 6. In general, the new prediction improves the prediction by Eq. (2) and Eq. (3) (i.e., lower RMSE and rMSE values) of these overtopping datasets.

One of the objectives of developing a new prediction is to improve the accuracy of Van der Meer and Bruce (2014) (Eq. (3)) for very small relative freeboards ($0 < R_c/H_{m0} < 0.11$) and zero freeboard ($R_c = 0$), which was consistently underpredicting the average overtopping rates within these cases for all the slope angles. Fig. 13 shows the new prediction (Eq. (15)) compared to Eq. (3) for the very small relative freeboard and zero freeboard cases of the fitting dataset, with Fig. 14 focuses only on the zero freeboard case. Eq. (15) shows an improvement of the accuracy of the prediction, as it adapts better than Eq. (3) to the data. As seen in Table 6, the RMSE value for very small relative freeboards of Eq. (15) is a 15% smaller for the range $0 < R_c/H_{m0} < 0.05$ than the RMSE value of Eq. (3), a 17% smaller for the range $0/05 < R_c/H_{m0} < 0.08$ and a 15% smaller for the range $0.08 < R_c/H_{m0} < 0.11$. For the zero freeboard case, the RMSE value of Eq. (15) is a 35% smaller than of Eq. (3). Moreover, for the zero freeboard case the variability of the measured data not explained by Eq. (15) (i.e., the rMSE) is 27.9%, while for Eq. (3) is 65.5% (a decrease of 57.4%).

Fig. 15 shows the comparison of the fitting dataset measured and predicted dimensionless average overtopping rates for Eq. (3) (top panel) and Eq. (15) (bottom panel). It is decided to show linear plots instead of logarithmic plots for a better visualization of the large overtopping rates. The line of perfect fit is shown in both panels, together with the 90% confidence band of the predictions (calculated with the RMSE value for all the tests of the fitting dataset, see Table 6). The data points below the perfect fit line are underestimated by the prediction, while the data points above the perfect fit line are overestimated by the prediction.

Eq. (3) shows a clear underestimation (in some cases outside the 90% confidence band) for the largest dimensionless overtopping rates which correspond to zero and very small relative freeboards, confirming the results discussed on Section 4.1. The overtopping rates for these conditions are better predicted by Eq. (15), with most of the values inside

the 90% confidence band. For larger relative crest freeboards both Eq. (3) and Eq. (15) are predicting correctly the overtopping rates, even though there are some outliers in the data.

The strength of Eq. (15) as a new overtopping prediction formula for steep low-crested structures is the size of the dataset used to fit the prediction and the use of the Ghent University datasets that are novel and that allow a better prediction of the overtopping on relative crest freeboard and slope angle ranges which before were a knowledge gap in the literature.

6. Conclusions

A new average overtopping prediction formulae (Eq. (15)) for steep low-crested structures under non-breaking conditions is obtained by fitting a Weibull-type formula through selected subsets of the CLASH database, the existing UG10 datasets, and the new UG13, UG14 and UG15 datasets obtained at Ghent University. The range of application of this formula is for structures with slope angles $0 \leq cot\ \alpha \leq 4$ and relative crest freeboards $R_c/H_{m0} \geq 0$ under non-breaking wave conditions. Only smooth and impermeable structures are included in the fitting dataset of the formula. The result is a prediction formula that improves the accuracy of the prediction by Van der Meer and Bruce (2014) (Eq. (3)) for the range of steep low-crested structures (slopes $2 > cot\ \alpha \geq 0$ with relative crest freeboards $0.8 > R_c/H_{m0} \geq 0$). The improved prediction accuracy by Eq. (15) compared to Eq. (3) is due to the new datasets featuring more than 900 overtopping tests of steep low-crested structures. The new datasets fill an overtopping data gap of steep low-crested structures that existed at the time when Eq. (3) was derived.

The prediction improvement is especially significant for zero freeboards ($R_c = 0$) (35% reduction of RMSE) and very small relative crest freeboards ($0.11 > R_c/H_{m0} > 0$) (16% reduction of RMSE), very steep slopes ($0.27 \geq cot\ \alpha > 0$) (31% reduction of RMSE) and vertical structures ($cot\ \alpha = 0$) (24% reduction of RMSE).

For vertical and composite vertical structures, the prediction of Eq. (15) is valid for vertical structures with or without influencing foreshores and for composite vertical structures without influencing
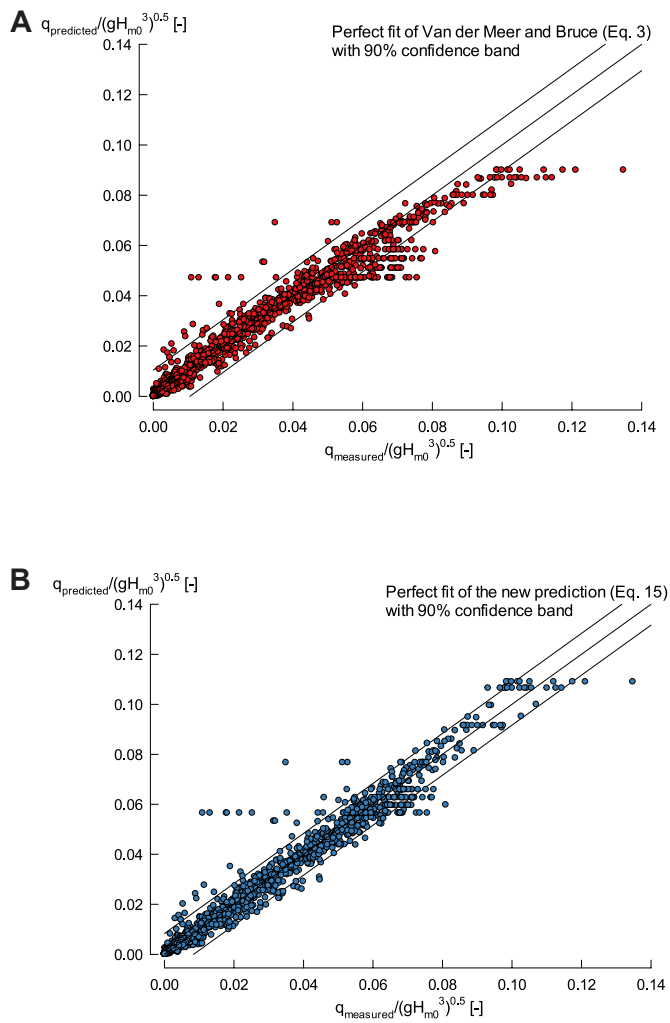
Fig. 15. Dimensionless average measured overtopping rate of the fitting dataset, compared with the dimensionless average predicted overtopping rate of Van der Meer and Bruce (2014) (Eq. (3)) on the top panel and the new prediction (Eq. (15)) on the bottom panel.

foreshores. This simplifies the decision chart for vertical structures suggested in Figure 7.2 of the EurOtop (2018) manual. For conventional structures (slopes $\cot \alpha \geq 2$ with relative crest freeboards $R_c / H_{m0} \geq 0.8$), Eq. (15) results in a very similar average overtopping prediction compared to Eq. (3) and the EurOtop (2007) manual prediction (Eq. (1)).

With the new UG13, UG14 and UG15 datasets it was possible to adapt better the prediction to the shape of the data, therefore obtaining an exponent for a Weibull-type formula of $c = 1.1$ (close to a straight line on a semilogarithmic plot) rather than $c = 1.3$ (a curved line on a semilogarithmic plot). New expressions of the influence factors γ_f and γ_β should be obtained for the new prediction, as the expressions already existing in literature (e.g., EurOtop (2018) manual) were fitted for the EurOtop (2007) prediction (Eq. (1)) with a $c = 1.0$. Using these published expressions of the influence factors γ_f and γ_β is possible for large relative crest freeboards as the error in the prediction is negligible. For small relative crest freeboards, the underprediction error due to these influence factors is smaller than 26%, which is within the 90% prediction band of the new prediction.

Compared to the Victor and Troch (2012a) (Eq. (2)) prediction, Eq. (15) has a very similar prediction accuracy for steep low-crested structures and also for conventional structures. This is due to the similar shape of both formulae in a semilogarithmic plot, being Eq. (2) bilinear and Eq. (15) slightly curved.

The following steps within this research are to analyse the individual overtopping volumes of the new datasets UG13, UG14 and UG15, in order to study its probability distribution and maximum volumes, proposing new prediction formulae valid for steep low-crested structures.

Credit author statement

David Gallach-Sánchez: Conceptualization, Methodology, Formal analysis, Investigation, Data curation, Writing - original draft, Visualization. Peter Troch: Conceptualization, Methodology, Writing - review & editing, Supervision, Project administration. Andreas Kortenhaus: Conceptualization, Methodology, Writing - review & editing, Supervision.

Declaration of competing interest

The authors declare that they have no known competing financial interests or personal relationships that could have appeared to influence the work reported in this paper.

Acknowledgements

Notation

a, b, c [$-$]   Coefficients in the three-parameter Weibull average overtopping prediction (Eq. (15))

a_{Victor}, b_{Victor} [$-$]   Coefficients in Eq. (2)

$a_{V\&B}, b_{V\&B}, c_{V\&B}$ [$-$]   Coefficients in Eq. (3)

g [m/s^2]   Acceleration due to gravity

h [m]   Water depth at the toe of the structure

H_{m0} [m]   Incident spectral wave height at the toe of the structure

m_{-1} [$-$]   First negative moment of the energy spectrum

m_0 [$-$]   Zeroth moment of the energy spectrum

N_{test} [$-$]   Number of tests

ODF [$-$]   Overtopping Discharge Factor as defined by Victor and Troch (2012a)

q [m^3/s/m]   Average overtopping rate

$q/\sqrt{gH_{m0}^3}$ [$-$]   Dimensionless average overtopping rate

q_{meas_n} [m^3/s/m] Average overtopping rate measured for the test n

q_{pred_n} [m^3/s/m]   Average overtopping rate predicted for the test n

R_c [m] Crest freeboard.

R_c/H_{m0} [−] Relative crest freeboard.

RF[-] Reliability factor

RMSE[-] Root mean square error given by Eq. (13)

rMSE[%] Relative mean square error given by Eq. (14)

RSS[-] Residual sum of squares given by Eq. (19)

$s_{m-1,0}$ [−] Wave steepness associated to $T_{m-1,0}$

$T_{m-1,0}$ [s] Spectral incident wave period defined by m_{-1}/m_0 at the toe of the structure

T_p [s] Peak incident wave period at the toe of the structure

$Var\left(\dfrac{q_{meas}}{\sqrt{gH_{m0}^3}}\right)$ [−] Variance of the dimensionless average overtopping measured for a specific set of data

α [°] Slope angle

β [°] Angle of oblique wave attack

γ [−] Shape parameter of the JONSWAP spectrum

γ_f [−] Influence factor on overtopping for roughness and permeability of the structure

γ_β [−] Influence factor on overtopping for oblique wave attack

μ [Var.] Average of a normally distributed parameter

$\xi_{m-1,0}$ [−] Surf similarity parameter (Iribarren number) associated to $T_{m-1,0}$

σ [Var.] Standard deviation of a normally distributed parameter

σ_{est} [Var.] Standard error of the estimate

σ' [−] Coefficient of variation $\sigma' = \sigma/\mu$ of a normally distributed parameter

References

Allsop, N.W.H., Besley, P., Madurini, L., 1995. Overtopping performance of vertical and composite breakwaters, seawalls and low reflection alternatives. Paper 4.7. In: EC FP3-MAST2 Monolithic (Vertical) Coastal Structures Project (MAS20047) Final Report. University of Hannover, Hannover, Germany.

Altomare, C., Suzuki, T., Chen, X., Verwaest, T., Kortenhaus, A., 2016. Wave overtopping of sea dikes with very shallow foreshores. Coast. Eng. 116, 236–257. https://doi.org/10.1016/j.coastaleng.2016.07.002.

Battjes, J.A., 1974. Computation of Set-Up, Longshore Currents, Run-Up and Overtopping Due to Wind-Generated Waves.. PhD thesis TU Delft.

De Rouck, J., Verhaeghe, H., Geeraerts, J., 2009. Crest level assessment of coastal structures - general overview. Coast. Eng. 56, 99–107. https://doi.org/10.1016/j.coastaleng.2008.03.014.

EurOtop, Van der Meer, J.W., Allsop, W., Bruce, T., De Rouck, J., Kortenhaus, A., Pullen, T., Schüttrumpf, H., 2018. Manual on Wave Overtopping of Sea Defences and Related Structures. An Overtopping Manual Largely Based on European Research, but for Worlwide Application. www.overtopping-manual.com.

EurOtop, Pullen, T., Allsop, W., Bruce, T., Kortenhaus, A., Schüttrumpf, H., Van der Meer, J.W., 2007. Wave Overtopping of Sea Defences and Related Structures: Assessment Manual. Kuratorium für Forschung im Küsteningenieurwesen, Hamburg, Germany.

Franco, L., de Gerloni, M., Van der Meer, J.W., 1994. Wave overtopping on vertical and composite breakwaters. In: ASCE (Ed.), Proceedings of the 24th International Conference on Coastal Engineering, pp. 1030–1045. https://doi.org/10.9753/icce.v24. New York, USA.

Gallach-Sánchez, D., 2018. Experimental Study of Wave Overtopping Performance of Steep Low-Crested Structures.. PhD thesis Ghent University.

Gallach-Sánchez, D., Illegems, M., Willems, Y., Troch, P., Kortenhaus, A., 2016. Experimental study of average overtopping performance on steep low-crested structures for shallow water conditions. In: Proceedings of the 6th International Conference on the Application of Physical Modelling in Coastal and Port Engineering and Science (Coastlab16). Ottawa, Canada.

Gallach-Sánchez, D., Troch, P., Kortenhaus, A., 2018. A critical analysis and validation of the accuracy of wave overtopping prediction formulae for OWECs. Energies 11, 133. https://doi.org/10.3390/en11010133.

Gallach-Sánchez, D., Troch, P., Vroman, T., Pintelon, L., Kortenhaus, A., 2014. Experimental study of overtopping performance of steep smooth slopes for shallow water wave conditions. In: Proceedings of the 5th Conference on the Application of Physical Modelling to Port and Coastal Protection (Coastlab14), pp. 334–343. Varna, Bulgaria.

Kortenhaus, A., Oumeraci, H., Geeraerts, J., De Rouck, J., Medina, J.R., González-Escrivá, J.A., 2004. Laboratory effects and further uncertainties associated with wave overtopping measurements. In: Proceedings of the 29th International Conference on Coastal Engineering, pp. 4456–4468. https://doi.org/10.1142/9789812701916-0359. Lisbon, Portugal.

Mansard, E.P.D., Funke, E.R., 1980. The measurement of incident and reflected spectra using a least squares method. In: Proceedings of the 17th International Conference on Coastal Engineering (ICCE 1980), pp. 154–172. https://doi.org/10.1061/9780872622647.008. Sidney, Australia.

Nørgaard, J.Q.H., Lykke Andersen, T., Burcharth, H.F., 2014. Distribution of individual wave overtopping volumes in shallow water wave conditions. Coast. Eng. 83, 15–23. https://doi.org/10.1016/j.coastaleng.2013.09.003.

Romano, A., Bellotti, G., Briganti, R., Franco, L., 2015. Uncertainties in the physical modelling of the wave overtopping over a rubble mound breakwater: the role of the seeding number and of the test duration. Coast. Eng. 103, 15–21. https://doi.org/10.1016/j.coastaleng.2015.05.005.

Schüttrumpf, H., 2001. Wellenüberlaufströmung bei Seedeichen. Experimentelle und theoretische Untersuchungen (in German) [Wave overtopping of sea dikes. An experimental and theoretical analysis].. PhD thesis Technischen Universität Braunschweig.

Smid, R., 2001. Untersuchungen zur Ermittlung der mittleren Wellenüberlaufrate an einer senkrechten Wand und einer 1:1,5 geneigten Böschung für Versuche mit und ohne Freibord (in German) [Analysis of the average overtopping discharge over a vertical wall and a 1:1.5 sloping structure for cases with and without freeboard].. PhD thesis Leichtweiss-Institut für Wasserbau, Technischen Universität Braunschweig.

TAW, 2002. Technical report wave run-up and wave overtopping at dikes. In: Technical Advisory Committee on Flood Defence, Delft, The Netherlands.

TAW, 1989. Leidraad Voor Het Ontwerpen Van Rivierdijken. Deel 2 - Benedenrivierengebied (In Dutch) [Guideline for Design of River Dikes. Part 2 - Lower Area]. Technical Advisory Committee on Flood Defence, Delft, The Netherlands.

Van der Meer, J.W., Bruce, T., 2014. New physical insights and design formulas on wave overtopping at sloping and vertical structures. J. Waterw. Port, Coast. Ocean Eng. 140 https://doi.org/10.1061/(ASCE)WW.1943-5460.0000221, 04014025–1, 04014025–18.

Van der Meer, J.W., Bruce, T., Allsop, W., Franco, L., Kortenhaus, A., Pullen, T., Schüttrumpf, H., 2013. EurOtop revisited. Part 1 : sloping structures. In: Proceedings of the ICE, Coasts, Marine Structures and Breakwaters. https://doi.org/10.1680/fsts.59757.0214. Edinburgh, United Kingdom.

Van der Meer, J.W., Janssen, J.P.F.M., 1994. Wave Run-Up and Wave Overtopping at Dikes and Revetments. Delft Hydraulics internal report, Delft, The Netherlands.

Van der Werf, I.M., Van Gent, M.R.A., 2018. Wave overtopping over coastal structures with oblique wind and swell waves. J. Mar. Sci. Eng. 6, 149. https://doi.org/10.3390/jmse6040149.

Van Gent, M.R.A., 1999. Physical Model Investigations on Coastal Structures with Shallow Foreshores. 2D Model Tests with Single and Double-Peaked Wave Energy Spectra. Delft Hydraulics report, Delft, The Netherlands.

Van Gent, M.R.A., Van den Boogaard, H.F.P., Pozueta, B., Medina, J.R., 2007. Neural network modelling of wave overtopping at coastal structures. Coast. Eng. 54, 586–593. https://doi.org/10.1016/j.coastaleng.2006.12.001.

Van Gent, M.R.A., Van der Werf, I.M., 2019. Influence of oblique wave attack on wave overtopping and forces on rubble mound breakwater crest walls. Coast. Eng. 151, 78–96. https://doi.org/10.1016/j.coastaleng.2019.04.001.

Verhaeghe, H., De Rouck, J., Van der Meer, J.W., 2008. Combined classifier-quantifier model: a 2-phases neural model for prediction of wave overtopping at coastal structures. Coast. Eng. 55, 357–374. https://doi.org/10.1016/j.coastaleng.2007.12.002.

Victor, L., 2012. Optimization of the Hydrodynamic Performance of Overtopping Wave Energy Converters: Experimental Study of Optimal Geometry and Probability Distribution of Overtopping Volumes.. PhD thesis Ghent University.

Victor, L., Troch, P., 2012a. Wave overtopping at smooth impermeable steep slopes with low crest freeboards. J. Waterw. Port, Coast. Ocean Eng. 138, 372–385. https://doi.org/10.1061/(ASCE)WW.1943-5460.0000141.

Victor, L., Troch, P., 2012b. Experimental study on the overtopping behaviour of steep slopes - transition between mild slopes and vertical walls. In: Proceedings of the 33rd International Conference on Coastal Engineering. ICCE 2012, Santander, Spain, pp. 1–23. https://doi.org/10.9753/icce.v33.structures.61.

Victor, L., Troch, P., 2010. Development of a test set-up to measure large wave-by-wave overtopping masses. In: Proceedings of the 3rd International Conference on the Applications of Physical Modelling to Port and Coastal Protection (Coastlab10), pp. 1–9. Barcelona, Spain.

Zanuttigh, B., Formentin, S.M., Van der Meer, J.W., 2016. Prediction of extreme and tolerable wave overtopping discharges through an advanced neural network. Ocean Eng. 127, 7–22. https://doi.org/10.1016/j.oceaneng.2016.09.032.

Zelt, J.A., Skjelbreia, J., 1992. Estimating incident and reflected wave fields using an arbitrary number of wave gauges. In: Proceedings of the 23rd International Conference on Coastal Engineering. ICCE 1992, pp. 777–789. https://doi.org/10.9753/icce.v23.%p.